Open access • Posted Content • DOI:10.1101/857839

The genomic landscape of intrinsic and acquired resistance to cyclin-dependent kinase 4/6 inhibitors in patients with hormone receptor positive metastatic breast cancer — Source link

Seth A. Wander, Ofir Cohen, Ofir Cohen, Xueqian Gong ...+33 more authors

Institutions: Harvard University, Broad Institute, Eli Lilly and Company, Cross Cancer Institute ...+1 more institutions

Published on: 28 Nov 2019 - bioRxiv (Cold Spring Harbor Laboratory)

Topics: Cancer cell and KRAS

The genomic landscape of intrinsic and acquired resistance to cyclin-dependent kinase 4/6 inhibitors in patients with hormone receptor positive metastatic breast cancer

Authors:
Seth A. Wander[£,1,2,3,4]
Ofir Cohen[£1,2,4]
Xueqian Gong[£, 5]
Gabriela N. Johnson[1,2,4]
Jorge Buendia-Buendia[1,2,4]
Maxwell R. Lloyd[1,2]
Dewey Kim[1,2,4]
Flora Luo[1,2,3,4]
Pingping Mao[1,2,3,4]
Karla Helvie[1,2]
Kailey J. Kowalski[1,2,4]
Utthara Nayar[1,2,3,4]
Adrienne G. Waks[1,2,3,4]
Stephen Parsons[5]
Ricardo Martinez[5]
Lacey M. Litchfield[5]
Xiang S. Ye[5]
Chun Ping Yu[5]
Valerie M. Jansen[5]
John R. Stille[5]
Patricia S. Smith[5]
Gerard J. Oakley[5]
Quincy Chu[6]
Gerald Batist[7]
Melissa Hughes[1,2]
Jill D. Kremer[5]
Levi A. Garraway[1,2,3,4,5]
Eric P. Winer[2,3]
Sara M. Tolaney[2,3]
Nancy U. Lin[2,3]
Sean Buchanan[5]
Nikhil Wagle[1,2,3,4]

1. Center for Cancer Precision Medicine, Dana-Farber Cancer Institute, Boston, MA
2. Department of Medical Oncology, Dana-Farber Cancer Institute, Boston, MA
3. Harvard Medical School, Boston, MA
4. Broad Institute of MIT and Harvard, Cambridge, MA
5. Eli Lilly and Co., Indianapolis, IN
6. Cross Cancer Institute, Alberta, Canada

7. Segal Cancer Centre, Jewish General Hospital, McGill University, Montreal, Canada

Running title:
Genomic mechanisms of CDK 4/6 inhibitor resistance in metastatic breast cancer

Key words: CDK 4/6, metastatic breast cancer, whole exome sequencing, aurora kinase, retinoblastoma

*Address correspondence to:
Nikhil Wagle, MD
Department of Medical Oncology
Dana-Farber Cancer Institute
450 Brookline Ave, Dana 820A
Boston, MA 02215
Phone: 617-632-6419
e-mail: nikhil_wagle@dfci.harvard.edu

£These authors contributed equally

Competing Financial Interest Statement

SAW has served as an advisor/consultant to Foundation Medicine (consulting); Eli Lilly (consulting); Puma Biotechnology (consulting); and InfiniteMD (consulting, equity) and receives institutional research funding from Genentech. AGW receives institutional research funding from Genentech and MacroGenics. QC receives institutional research funding from Abbvie, Amgen, Astra Zeneca, Aurka, Boheringer Ingelheim, BMS, Celgene, Debio, Esparas, Eli Lilly, GSK, Merck, Novartis, Roche, TP Therapeutics; as well as advisory fess and hororaria from Abbvie, Astra Zeneca, Bohehringer Ingelheim, BMS, Eli Lilly, Merck, Novartis, Roche, Takeda. SMT has received institutional research support from Merck, Bristol-Myers Squibb, Exelixis, Eli Lilly, Pfizer, Novartis, AstraZeneca, Eisai, Nektar, Odenate, Sanofi, Immunomedics, Cyclacel, and Genentech; and has served as a consultant/advisor for Genentech, Eli Lilly, Novartis, Pfizer, Celldex, Paxman, Seattle Genetics, Nektar, Immunomedics, Nanostring, Daiichi-Sankyo, Bristol-Meyers Squibb, Sanofi, Abbvie, Athenex, AstraZeneca, Eisai, Puma, and Merck. NUL is a consultant for Puma Biotechnology, Seattle Genetics, and Daichii Sankyo, and received institutional research funding from Merck, Pfizer, Genentech, Array Biopharma, Novartis and Seattle Genetics. EPW has served as a consultant/advisor for InfiniteMD, Genentech, and Eli Lilly. NW was previously a stockholder and consultant for Foundation Medicine; has been a consultant/advisor for Novartis and Eli Lilly; and has received sponsored research support from Novartis and Puma Biotechnology. XG, SP, RM, LML, XSY, CPU, GJO, VMJ, JRS, PSS, LAG, and SB were employees and shareholders of Eli Lilly and Company at the time of manuscript preparation. Except as indicated by the author affiliations, none of these entities had any role in the conceptualization, design, data collection, analysis, decision to publish, or preparation of the manuscript.

Abstract

Clinical resistance mechanisms to CDK4/6 inhibitors in HR+ breast cancer have not been clearly defined. Whole exome sequencing of 59 tumors with CDK4/6i exposure revealed multiple candidate resistance mechanisms including *RB1* loss, activating alterations in *AKT1*, *RAS*, *AURKA*, *CCNE2, ERBB2,* and *FGFR2,* and loss of ER expression. *In vitro* experiments confirmed that these alterations conferred CDK4/6i resistance. Cancer cells cultured to resistance with CDK4/6i also acquired *RB1*, *KRAS*, *AURKA*, or *CCNE2* alterations, which conferred sensitivity to AURKA, ERK, or CHEK1 inhibition. Besides inactivation of RB1, which accounts for ~5% of resistance, seven of these mechanisms have not been previously identified as clinical mediators of resistance to CDK4/6 inhibitors in patients. Three of these—RAS activation, AKT activation, and AURKA activation—have not to our knowledge been previously demonstrated preclinically. Together, these eight mechanisms were present in 80% of resistant tumors profiled and may define therapeutic opportunities in patients.

Significance

We identified eight distinct mechanisms of resistance to CDK4/6 inhibitors present in 80% of resistant tumors profiled. Most of these have a therapeutic strategy to overcome or prevent resistance in these tumors. Taken together, these findings have critical implications related to the potential utility of precision-based approaches to overcome resistance in many patients with HR+ MBC.

Introduction

The cyclin-dependent kinase 4/6 inhibitors (CDK4/6i) have entered widespread use in both the first- and subsequent-line setting for patients with hormone-receptor positive (HR+), human epidermal growth factor receptor 2 negative (HER2-) metastatic breast cancer (MBC).[1,2] Their application has resulted in significant improvements in progression-free survival (PFS) and overall survival (OS) for treatment-naïve and previously treated patients in combination with anti-estrogens.[3-9] Abemaciclib has shown efficacy as a single agent in endocrine-refractory disease, and has been approved for use as monotherapy in pre-treated patients with HR+/HER2- MBC.[10] Despite these advances, HR+/HER2- MBC remains a significant cause of morbidity and mortality. Many patients demonstrate *de novo*, or intrinsic, resistance to these agents and, in those who respond, acquired resistance and disease progression is unfortunately inevitable.

We have limited insight into the molecular pathways governing resistance to CDK4/6i. Early development of these compounds indicated preferential efficacy in luminal/Rb-positive cell lines.[11] Loss of Rb expression has been identified in cellular models cultured to resistance in CDK4/6i.[12] Acquired *RB1* loss-of-function mutations were identified in circulating tumor DNA (ctDNA) from three patients following progression on CDK4/6i-based therapy.[13] Analysis of ctDNA from patients treated on the PALOMA-3 trial, which explored palbociclib with fulvestrant versus fulvestrant alone in the second-line metastatic setting, demonstrated rare *RB1* mutations that were uniquely present in the group

140 receiving palbociclib.[14] *PIK3CA* and *ESR1* mutations were identified frequently
141 on both arms of the study, and neither has been well established as a predictive
142 biomarker.[14,15] Recent analysis of ctDNA and tumors from the MONARCH-2
143 study, exploring abemaciclib and fulvestrant in patients with prior progression on
144 anti-estrogen therapy, suggested benefit from abemaciclib use regardless of
145 *PIK3CA* or *ESR1* status, though the magnitude of benefit was larger in mutant
146 patients.[16] Despite lack of robust data supporting a role for PI3K, loss of the
147 *PTEN* tumor suppressor was recently noted in tumor samples with progression
148 on ribociclib, and was sufficient to promote resistance *in vitro*.[17] Preclinically,
149 PDK1, another PI3K pathway effector, emerged from a kinome-wide screen in
150 HR+ cells as a potential mediator of resistance to CDK4/6i; targeting PDK1 or
151 PI3K prompted resensitization to CDK4/6i.[18]
152
153 Preclinical studies have also implicated overexpression of CDK6 and cyclin E2
154 (CCNE2) in mediating resistance.[19,20] Increased expression of cyclin E1
155 (CCNE1) was associated with inferior response to palbociclib on PALOMA-3,
156 while the expression of cyclin D1, RB1, and CDK4 failed to demonstrate any
157 association.[21] Targeted sequencing of tumor specimens from patients with HR+
158 MBC and CDK4/6i exposure suggested that regulation of CDK6 expression via
159 the FAT1 tumor suppressor could provoke resistance[22] and CDK6 expression
160 may also be regulated via micro-RNA-dependent modulation of the TGF-B
161 pathway, altering sensitivity to CDK4/6i *in vitro* and in patients.[23]
162

Prior work from our laboratory has implicated alterations in *ERBB2* and *FGFR2* in mediating resistance to CDK4/6i *in vitro* and in patients.[24,25] In addition, amplification of *FGFR1*, identified via sequencing of ctDNA from MONALEESA-2 (ribociclib and anti-estrogen in the first-line metastatic setting), correlated with reduced PFS and activation of FGFR1 provoked resistance *in vitro.*[26]

Here we explore the genomic landscape of resistance to CDK4/6i via whole exome sequencing of tumor biopsies. The landscape of resistance to CDK4/6i is heterogeneous, with multiple potential mediators including biallelic *RB1* disruption and activation of *AKT1*, *RAS*, *ERBB2*, *FGFR2*, Aurora Kinase A (*AURKA*), and *CCNE2*. Modification of HR+ breast cancer cells, via CRISPR-mediated knockout or lentiviral overexpression, corroborates the candidate mechanisms of resistance identified by tumor sequencing. Cells cultured to resistance in the presence of CDK4/6i demonstrate concordant alterations in RB1, AURKA, and CCNE2 expression along with RAS/ERK activation and demonstrate enhanced sensitivity to novel targeted therapies. In one patient with HR+/HER2- MBC that progressed on first-line CDK4/6i, AURKA inhibition provoked prolonged disease control in a phase I clinical trial. These results shed new light on the diverse landscape of genomic alterations that drive resistance to CDK4/6i in HR+/HER2- MBC and provide preclinical and translational rationale for novel strategies to circumvent and overcome resistance.

Results

The genomic landscape of intrinsic and acquired CDK4/6i resistance

We identified patients with HR+/HER2- MBC who were treated with CDK4/6i with or without an anti-estrogen and provided metastatic tumor biopsies as part of an IRB-approved tissue collection protocol.[27] We classified samples as reflecting sensitivity, intrinsic resistance, or acquired resistance (Figure 1A). Sensitive biopsies were defined as baseline samples obtained within 120 days prior to, or up to a maximum of 31 days after, CDK4/6i initiation in a patient with subsequent clinical benefit (defined as radiographic response or stable disease >6 months). Biopsies reflecting intrinsic resistance were obtained within 120 days prior to or anytime after CDK4/6i initiation in patients without evidence of clinical benefit (defined as progression on the first interval restaging study or stable disease <6 months). Biopsies reflecting acquired resistance were obtained from patients who had experienced clinical benefit with CDK4/6i and had an available biopsy specimen within 31 days prior to progression or at any time thereafter.

WES was successfully performed on 59 biopsies from 58 patients within the appropriate exposure window to be assigned a phenotype and with sufficient clinical data to define response (Supplemental Table 1). This included 18 sensitive biopsies, 28 intrinsic resistance biopsies, and 13 acquired resistance biopsies. The majority of patients (55, 94.8%) received standard combinations of an aromatase inhibitor or fulvestrant and a CDK4/6 inhibitor. 49 patients (84.5%) received a palbociclib-based regimen, including 28 patients (48.3%) with an

208 aromatase inhibitor and 20 patients (34.5%) with fulvestrant. The mean duration
209 of therapy was 316 days (range 43-1052). Patients received an average of 1.5
210 lines of therapy in the metastatic setting (range 0-7) and 30 patients (51.7%) had
211 prior anti-estrogen exposure in the metastatic setting. Additional clinical
212 parameters are described in Supplemental Table 2.
213
214 Whole exome sequencing of all 59 samples demonstrated a number of genomic
215 alterations in genes implicated in HR+ breast cancer (*ESR1, PIK3CA, CCND1,*
216 *FGFR1, TP53*) as well as additional cancer genes and putative resistance
217 mediators (*RB1, ERBB2, FGFR2, AKT1, KRAS, HRAS, NRAS*, among others)
218 (Figure 1B, Supplemental Table 3). Many of these alterations were enriched in
219 resistant samples and not present or relatively infrequent in sensitive samples,
220 suggesting they might be contributing to resistance (Figure 1B; Supplemental
221 Figure 1; Supplemental Table 4). In addition to these genomic differences, three
222 patients with resistant tumor biopsies demonstrated loss of ER expression in the
223 metastatic drug-resistant tumor (measured by immunohistochemistry); all
224 patients were known to be ER+ at the time of metastatic diagnosis.
225
226 While isolated amplification events were identified in a variety of cancer genes
227 (Supplemental Table 4), amplification events in aurora kinase A were observed
228 as occurring more frequently in resistant samples as compared with sensitive (0
229 in sensitive, 26.8% in resistant; 0.0081, Welch test) (Figure 1C). While only
230 moderate magnitude AURKA amplifications were seen among the resistant

231 tumors, in The Cancer Genome Atlas (TCGA) study, even low AURKA
232 amplification in primary HR+ breast cancer samples resulted in a statistically
233 significant increase in gene expression (Supplementary Figure 2), suggesting
234 that the degree of AURKA amplification observed in the CDK4/6i-resistant cohort
235 is likely to have a meaningful effect on gene expression and protein level.
236
237 Based on prior preclinical studies and known biology, we hypothesized that the
238 following eight specific categories of alterations that were enriched in the
239 resistant tumors were contributing to CDK4/6i resistance: biallelic disruption of
240 *RB1*, activating mutation and/or amplification of *AKT1*, activating mutations in
241 *KRAS/HRAS/NRAS*, activating mutations and/or amplification of *FGFR2*,
242 activating mutations in *ERBB2*, amplification of CCNE2, amplification of AURKA,
243 and loss of ER.
244
245 In total, 33 out of the 41 resistant biopsies (80.5%) had genomic alterations in at
246 least one of these 8 potential resistance mechanisms, as compared to 3 of the 18
247 sensitive biopsies (Figure 1D, Supplemental Table 5). Consistent with prior
248 reports, biallelic disruption in *RB1* was exclusively present in resistant samples
249 and occurred in a minority of resistant biopsies (n=4/41, 9.8%). We identified
250 diverse mechanisms of biallelic *RB1* disruption across the affected patients. In all
251 examples, a single copy loss was noted in the presence of a point mutation,
252 splice site alteration, or frameshift event in the second allele.
253

AKT1 alterations were identified in five resistant biopsies (n=5/41, 12.2%), including both mutational events and amplifications. A single sensitive biopsy also demonstrated an activating AKT1 alteration (n=1/18, 5.6%).

Diverse RAS-pathway activating events were observed in four CDK4/6i-resistant cases (n=4/41, 9.8%) including canonical activating mutations in *KRAS* G12D, a pathogenic mutation in KRAS Q61L,[28] a mutation in *HRAS* K117N,[29] and high focal amplification in *NRAS* (Figure 1B). There were no instances of RAS-altered tumors with a sensitive phenotype.

Amplification events in AURKA were identified in eleven resistant biopsies (n=11/41, 26.8%), including examples of both intrinsic and acquired resistance (n=7 and n=4, respectively). There were no sensitive biopsies with AURKA amplification.

There were six instances (n=6/41, 14.6%) of CCNE2 amplification identified across the resistant cohort (Figure 1B). A single sensitive biopsy with a CCNE2 alteration was identified (n=1/18, 5.6%).

FGFR2 alterations were noted in three resistant biopsies (all with intrinsic resistance) (n=3/41, 7.3%), while activating mutations or amplification of ERBB2 was noted in five resistant biopsies (n=5/41, 12.2%). A single sensitive biopsy with an ERBB2 alteration was also identified (n=1/18, 5.6%).

277

278 With respect to ER signaling, three resistant biopsy samples exposed to CDK4/6i
279 and an anti-estrogen demonstrated loss of ER expression via IHC (n=3/41,
280 7.3%); there were no patients with ER loss among the sensitive tumor samples
281 (Figure 1B; Supplemental Table 5). These results support pre-clinical work
282 suggesting CDK4/6i was predominantly effective in HR+ luminal cell lines while
283 HR- basal cell lines demonstrated frequent intrinsic resistance.[11]

284

285 Enrichment in *ESR1* mutations was appreciated amongst resistant tumors
286 (n=14/41, 34.1%; Supplemental Table 4) compared to sensitive tumors (n=3/18,
287 16.7%). *ESR1* mutations among sensitive tumors occurred exclusively in patients
288 receiving fulvestrant and were not found in patients who achieved clinical benefit
289 with CDK4/6i and an aromatase inhibitor, as would be expected (Supplementary
290 Figure 1).[30] These results support the notion that *ESR1* mutations are frequently
291 acquired during the development of endocrine resistance, while also suggesting
292 that they are not sufficient to drive simultaneous resistance to CDK4/6i.

293

294 Notably, mutational events in *PIK3CA* occurred frequently in both sensitive
295 (n=8/18, 44.4%) and resistant (n=18/41, 43.9%) specimens, suggesting that
296 *PI3KCA* is unlikely to be a marker of resistance. Copy number gains in *FGFR1*
297 were also noted amongst both sensitive (n=4/18, 22.2%) and resistant biopsies
298 (n=4/41, 9.8%).

299

Systematic differences in the relative proportion of these alterations were not apparent when comparing the intrinsic and acquired resistance subgroups, although the power of this analysis is limited by sample size (Figure 1D, Supplemental Table 4).

Evolutionary dynamics in acquired CDK4/6i resistance

Matched pre- and post-treatment samples were available from seven patients who experienced acquired resistance to CDK4/6i. We compared the WES from the paired pre-treatment and post-treatment samples and performed an evolutionary analysis to evaluate clonal structure and dynamics, including changes in mutations and copy number. We established the evolutionary classification of each mutation to distinguish events that were acquired or enriched in clones that are dominant in the post-progression tumor, as compared with the pre-treatment counterpart (Figure 2, Supplemental Table 6).

Potential drivers of resistance that are observed in evolutionary acquired clones included a biallelic *RB1* disruption (Figure 2A), an *AKT1* amplification (Figure 2B), an *AKT1* activating mutation (Figure 2D), and an *ESR1* activating mutation (Figure 2G).

In the patient with biallelic *RB1* disruption and an available matched pair for exome analysis, the pre-treatment specimen demonstrated a single copy deletion in *RB1*. Two separate post-progression biopsy samples demonstrated unique

323 alterations in the second copy of *RB1,* suggesting convergent evolution toward a
324 common mechanism of resistance within the same tumor ecosystem (Figure 2A).
325
326 Genomic diversity was also observed in various mechanisms of AKT activation.
327 In two patients with matched pre/post-treatment exome pairs, we observed
328 acquisition of a pathogenic *AKT1* point mutation (*W80R*)[31-33] (Figure 2D) and
329 acquisition of an *AKT1* copy-number amplification (Figure 2B). Taken together,
330 these cases suggest that cancer clones with activated AKT by either pathogenic
331 mutation or high copy-number can confer selective advantage under CDK4/6i
332 treatment.
333
334 In four of these pairs, the mechanism of acquired resistance remains unclear.
335 We did not identify any instances of acquired AURKA overexpression, RAS
336 activation, or CCNE2 amplification, though the analysis was limited by number of
337 available matched pairs.
338
339 **Clinical case histories of patients with CDK4/6 inhibitor resistance**
340 Figure 3 illustrates the clinical details of selected patients with intrinsic and
341 acquired resistance to CDK4/6i and putative driver alterations. These include four
342 instances of biallelic RB1 disruption (Figure 3A), three patients with AKT1
343 activation (Figure 3B), three with RAS activation (Figure 3C), and three with high
344 CCNE2 amplification (Figure 3D).
345

Supplemental Figure 3 illustrates the three sensitive biopsy counter-examples: a single instance of AKT1 activation (Supplemental Figure 3A), a patient with low-level CCNE2 amplification (Supplemental Figure 3B), and a single ERBB2 alteration, all with clinical benefit on CDK4/6i (Supplemental Figure 3C).

Given the prominent (or exclusive) enrichment of *RB1* disruption, *AKT1* activation, RAS mutation, *AURKA* amplification, and *CCNE2* amplification within samples demonstrating resistance to CDK4/6i, we opted to pursue additional molecular validation of these targets. Prior work from our group and others implicating *FGFR* pathway and *ERBB2* activation in CDK4/6i resistance have been reported elsewhere.[24-26]

Candidate alterations provoke resistance to CDK4/6i and anti-estrogens *in vitro*

T47D and MCF7 HR+/HER2- breast cancer cells were utilized to explore whether these five genetic alterations confer resistance to CDK4/6i *in vitro*. *AKT1*, *KRAS G12D*, *AURKA,* and *CCNE2* were overexpressed via lentiviral transduction; *RB1* was inactivated via CRISPR-mediated knockout (Figure 4A; Supplemental Figure 4A). The impact of these alterations on susceptibility to CDK4/6 inhibitors was examined. Consistent with sequencing results, all alterations were sufficient to cause resistance to either palbociclib or abemaciclb in T47D cells (Figure 4B-F). Corresponding IC50 estimates for each dose-response curve are provided (Supplemental Table 7). Similar results were obtained in MCF7 cells

(Supplemental Figure 3), though AURKA did not provoke resistance to CDK4/6i in this cell line, suggesting that context dependence may explain differences between cell lines, as with biopsies.

Given that most patients in the clinic are treated with a combination of CDK4/6i and an anti-estrogen, we also explored sensitivity to fulvestrant (Supplemental Figure 5). Cells lacking RB1 were only minimally resistant to fulvestrant monotherapy in both T47D and MCF7. Both AKT1 and CCNE2 overexpression conveyed resistance to fulvestrant in T47D and MCF7. Both KRAS G12D and AURKA overexpression provoked significant resistance to fulvestrant in T47D cells and but not in MCF7 cells.

Taken together, these results underscore the biological complexity related to the emergence of clinical resistance to these drug combinations both *in vitro* and in patients. They suggest that the resistance mechanisms identified in patient samples may provoke differential resistance to the CDK4/6- and estrogen-based components of the treatment regimen, and that these effects may depend upon additional cell-specific features.

Resistance mediators arise independently during culture to resistance and define new dependencies *in vitro*

Given the results identified via exogenous manipulation of the mediators described above, we sought to explore resistance to CDK4/6i via orthogonal

platforms in the laboratory. The HR+ cell lines T47D, MCF7, and MDA-MB-361 were cultured to resistance in the presence of increasing doses of palbociclib or abemaciclib. To examine whether the putative drivers identified in patients were also responsible for resistance under selection *in vitro*, we characterized the resistant derivatives for levels of retinoblastoma protein, aurora kinase, cyclin E2 and for activated effectors of KRAS or AKT1 (Figure 5A).

Many of the putative resistance drivers identified via patient sequencing emerged spontaneously under selective pressure *in vitro*. 361-AR-1 (a derivative of MDA-MB-361 cells cultured to resistance in abemaciclib) was found to have an oncogenic *KRAS G12V* mutation (data not shown) and demonstrated increased ERK activation (Figure 5A). Proteomic analysis showed activation of multiple MAPK pathway components, including ERK, MEK and RSK (Supplemental Figure 6). T47D-AR-1 (a derivative of T47D cells cultured to resistance in abemaciclib) demonstrated decreased RB1 along with increased AURKA and pERK (Figure 5A). 361-PR-1 (a derivative of MDA-MB-361 cells cultured to resistance in palbociclib) demonstrated increased AURKA and CCNE2 protein levels (Figure 5A). Finally, MCF7-PR-1 (a derivative of MCF7 cells cultured to resistance in palbociclib) demonstrated increased expression of CCNE2 (Figure 5A). All derivative cell lines were confirmed to be resistant to abemaciclib compared with their parental counterparts (Figure 5B).

Therapeutic approaches are suggested by alterations identified in patient tumor specimens and cell lines cultured to resistance (Figure 5C). 361-AR-1 cells demonstrated increased KRAS/ERK activity and enhanced sensitivity to LY3214996, a selective ERK inhibitor. Both AURKA-amplified and RB1-low cells (T47D-AR-1 and 361-PR-1) were highly sensitive to LY3295668, a novel and selective AURKA inhibitor that has previously been reported to show synthetic lethality with RB1 loss.[34] Finally, cancers with high cyclin E and CDK2 activation have been reported to be dependent on CHEK1.[35] CCNE2-amplified cells (MCF7-PR-1) were highly sensitive to prexasertib, a CHEK1 inhibitor. Corresponding IC50 values for CDK4/6i and targeted agent treatment for these cell lines are included in Supplemental Table 8.

When compared to tumor sequencing results from patients with progression on CDK4/6i, the spontaneous emergence of corresponding alterations *in vitro* lends further support to the roles RB1 loss, RAS activation, CCNE2 overexpression, and AURKA overexpression may play in mediating resistance. That these alterations arose in parallel in different cancer cell lines (akin to different patients) also supports the earlier observation that cellular context may dictate which alterations arise under selective pressure via CDK4/6i. These results suggest that, in the presence of specific driver alterations in resistant tumor cells, unique dependencies may emerge which could inform novel therapeutic strategies.

436 **AURKA inhibition resulted in prolonged clinical benefit in a patient with**
437 **HR+/HER2-, RB1+ MBC following progression on CDK4/6i-based therapy**

438 LY3295668, the same AURKA specific inhibitor utilized *in vitro* to demonstrate a
439 new dependence on AURKA in MDA-MB-361 and T47D cells cultured to
440 resistance in CDK4/6i (Figure 5B, C), has entered early-stage clinical trials
441 (NCT03092934).

442

443 As a proof-of-concept example, we provide the case history of a patient with
444 locally advanced HR+/HER2- breast cancer treated on the trial. She had
445 chemotherapy and adjuvant tamoxifen prior to metastatic recurrence; at that
446 time, she was treated with first-line palbociclib and letrozole (Figure 6A). After
447 prolonged clinical benefit on this regimen (>3 years), she progressed and
448 enrolled on study with LY3295668. Her first restaging studies demonstrated
449 disease stability, which persisted for approximately 11 months (Figure 6A, top).
450 Immunohistochemical staining of her pre-treatment liver biopsy following
451 progression on CDK4/6i demonstrated high levels of the proliferative marker Ki67
452 and high RB1 protein expression (Figure 6A, bottom), suggesting the mechanism
453 of sensitivity to AURKA inhibition was not due to Rb loss. Sufficient additional
454 biopsy material was not available for further sequencing or IHC-based analysis at
455 the time of this writing. Our results lead us to speculate that sensitivity to AURKA
456 inhibition in this patient could be due to alternative resistance mechanisms, such
457 as AURKA amplification.

Discussion

CDK4/6 inhibitors, in combination with an anti-estrogen, have emerged as the standard of care for HR+/HER2- MBC. Despite widespread use, we have limited understanding of the mechanisms governing resistance and deciphering that landscape constitutes a critically important unmet need. To our knowledge, we provide the first analysis based upon whole exome sequencing of sensitive and resistant tumor tissues in a diverse cohort of patients who received CDK4/6i. This effort confirmed previous reports implicating rare events in RB1 while also revealing novel mediators of resistance including AKT1, RAS family oncogenes, AURKA, CCNE2, and ER loss. Prior work from our group and others identified mutational events in ERBB2[25] and the FGFR pathway[24,26,36] in driving resistance. *In vitro* experiments confirm that AKT1, KRAS G12D, AURKA, and CCNE2 confer resistance to CDK4/6i. RB1 downregulation, RAS/ERK activation, AURKA overexpression, and/or CCNE2 overexpression emerged spontaneously with prolonged CDK4/6i exposure, lending further support to their putative role as resistance effectors. These alterations correspond with the emergence of novel dependencies *in vitro*, providing therapeutic rationale for new targeted strategies in the clinic (Figure 6B). Finally, we provide an example of sustained clinical benefit with a novel AURKA inhibitor in a patient with HR+/HER2- MBC following progression on CDK4/6i.

Despite its central role downstream of CDK4/6, alterations in RB1 were observed only in a minority of patients who developed resistance to CDK4/6i. Anecdotal

481 evidence of acquired alterations in RB1 at the time of progression was provided
482 via ctDNA sequencing in three patients with exposure to CDK4/6i.[13] ctDNA
483 analysis from 195 patients treated on the PALOMA-3 study with fulvestrant and
484 palbociclib also demonstrated rare RB1 alterations (~5%), uniquely enriched in
485 the palbociclib-containing arm.[14] Relatively frequent driver alterations in *PIK3CA*
486 and *ESR1* were also identified, though occurred in both treatment groups on
487 PALOMA-3. These results were consistent with a recent study in which pre-
488 treatment biopsies were subjected to targeted sequencing; alterations in RB1
489 were again rare (~3%) and were associated with significantly impaired PFS on
490 CDK4/6i.[22] Our data supports the notion that RB1 alterations occur in a minority
491 of CDK4/6i-resistant patients (4/41, ~9.8%) and we provide new insight into
492 diverse mechanisms of biallelic disruption. In a single patient with multiple pre-
493 and post-treatment biopsies, two distinct mechanisms of biallelic inactivation
494 were identified in separate post-progression biopsies, demonstrating convergent
495 evolution under selective pressure for tumors with single copy loss *in vivo*. These
496 findings were supported by culture to resistance experiments, in which multiple
497 cell lines downregulated RB1 expression under selective pressure. While the rate
498 of genomic RB1 disruption in tumor samples appears to be low following
499 progression, additional non-genomic events may be missed by targeted or
500 exome-based sequencing (such as methylation, mutations in regulatory regions,
501 or post-translational modification). These possibilities warrant additional study.
502

Prior efforts suggested that common alterations in *CCND1*, *PIK3CA*, and *ESR1* did not impact PFS on CDK4/6i. We did not find an association between *CCND1*, *PIK3CA*, or *ESR1* alterations and CDK4/6i resistance in tumor specimens. Of note, alterations in *TP53* were enriched in CDK4/6i resistant biopsies. Mutant *TP53* is not sufficient to promote resistance to CDK4/6i *in vitro* as MCF7 (*TP53* wild-type) and T47D (*TP53* mutant) are both sensitive at baseline. Enrichment of *TP53* mutation in resistant specimens may result from heavier pre-treatment (including chemotherapies), may be permissive for the development of other resistance-promoting alterations, or may cooperate with secondary alterations to drive CDK4/6i resistance *in vivo*. The role of TP53 in CDK4/6i resistance remains an active area of research in the laboratory.

Several lines of evidence suggest CDK6 as a potential mechanism of resistance to CDK4/6 inhibitors.[19] While clinical studies have not identified any examples of CDK6 alterations in resistant samples, a recent study that performed targeted sequencing in 348 tumor specimens obtained prior to treatment with CDK4/6i demonstrated that loss of function mutations in the *FAT1* tumor suppressor resulted in resistance to CDK4/6i. Interestingly, *FAT1* was shown to result in upregulation of CDK6 expression via the Hippo pathway *in vitro.*[22]. Finally, recent work from our institution demonstrated that micro-RNAs modulate CDK6 expression via the TGF-B pathway to alter sensitivity to CDK4/6i *in vitro.*[23] Increased expression of the implicated miRNA (432-5p) correlated with resistance in a subset of the breast cancer patients exposed to CDK4/6i from the

526 cohort analyzed here.[23] In our study, we did not find examples of activating
527 events in CDK6, nor did we identify *FAT1* alterations amongst resistant samples.
528 Deletion and truncation mutations in *FAT1* appear to be extremely rare (reported
529 in 6 of 348 patients in *Li et al*).[22] Given their very low frequency and our sample
530 size (n=58 patients), our study was likely not sufficiently powered to identify this
531 rare event.
532
533 Unlike ctDNA-based targeted sequencing reported from the PALOMA-3 study,
534 the cohort analyzed here represents, to our knowledge, the first analysis based
535 upon whole exome sequencing from clinically annotated biopsies reflecting a
536 diverse group of patients with exposure to multiple CDK4/6i-based regimens. In
537 addition to expected alterations in RB1, we identified a heterogeneous landscape
538 of resistance, in which a variety of rare driver events span a diverse spectrum of
539 potential mediators. We confirm enrichment of activating mutations in *ERBB2*
540 and amplification events in *FGFR2* in resistant patients, and both pathways
541 provoke resistance to anti-estrogens and CDK4/6i *in vitro.*[24-26,36] We present, to
542 our knowledge, the first evidence implicating AKT1, RAS, and AURKA in
543 mediating resistance to CDK4/6i in patients. Targeted sequencing of ctDNA via
544 samples from PALOMA-3 also identified rare events in *ERBB2*, *AKT1*, *KRAS*,
545 and *FGFR2* which were both acquired and maintained at progression, however
546 this analysis was limited by lack of insight into the clinical response phenotype of
547 these samples.[14] We would hypothesize that “maintained” alterations identified in
548 the context of that study represent instances of early- or intrinsic resistance while

549 "acquired" alterations are more likely to arise in patients with transient response
550 or clinical benefit from CDK4/6i. CCNE2 and AURKA did not emerge as potential
551 resistance mediators in that study, likely due to lack of insight into copy number
552 alterations as a result of the sequencing methodology.
553
554 More recent correlative analyses from PALOMA-3 suggested that CCNE1
555 expression is associated with inferior outcome for patients receiving palbociclib.[21]
556 While we did not see examples of CCNE1 amplification in this cohort, we do
557 provide, to our knowledge, the first evidence that CCNE2 amplification is also
558 associated with the resistant phenotype. Of note, given its proximity to the
559 centromere, copy number analysis of CCNE1 via WES is technically challenging
560 and this may have resulted in under-estimation of amplification events in this
561 gene.
562
563 While all of these mediators provoked resistance to CDK4/6i *in vitro*, in specific
564 instances there were cell-line-dependent differences in their ability to circumvent
565 CDK4/6i. This notion of context-specificity is supported by several isolated
566 counter-examples in patients, in which putative resistance mediators were found
567 to occur in individual patients who derived at least transient clinical benefit from
568 CDK4/6i. These findings are also consistent with the spontaneous emergence of
569 distinct resistance mediators in specific cell lines – for example, RAS/ERK-
570 activated and AURKA-amplified cells emerged in MDA-MB-361 but not in MCF7,
571 and exogenous overexpression of AURKA could not provoke resistance in

572 MCF7. The situation is further complicated by variation in anti-estrogen
573 resistance *in vitro*. As an example, AKT1 overexpression may be sufficient to
574 provoke resistance to both CDK4/6i and fulvestrant, while alterations in RB1 may
575 require a second cooperative event to overcome the anti-estrogen component of
576 the regimen (such as *ESR1* alteration). These nuances underscore the
577 complexity of modeling resistance to therapeutic combinations *in vitro* and
578 highlight the need for additional studies to explore context-specific factors, which
579 might dictate the emergence of resistance with a potential driver of interest.
580
581 The majority of alterations identified in our clinical cohort, and confirmed *in vitro*,
582 are amenable to therapeutic intervention via emerging agents (Figure 6B). These
583 results suggest that a non-selective regimen is unlikely to yield reliable clinical
584 benefit, while a precision-based approach, informed by the underlying genomic
585 findings at progression, could guide selection of therapy in CDK4/6i-resistant
586 patients. RAS-activated cells that emerged under selective pressure with
587 CDK4/6i were highly sensitive to LY3214996, a selective ERK inhibitor. The
588 CHEK1 kinase plays well-established roles in regulating cell cycle progression in
589 the setting of DNA damage.[37] Cancer cells with replication stress caused by
590 activated CDK2 appear to be particularly sensitive to Chk inhibitors[38] and *CCNE1*
591 amplification has been linked to CHEK1 dependence.[35] HR+ cells expressing
592 high levels of CCNE2 demonstrated enhanced sensitivity to prexasertib, a
593 CHEK1 inhibitor that has been well tolerated in human patients with early
594 evidence suggesting clinical efficacy in a phase I study.[39]

595

596 The aurora kinases regulate organization of the mitotic spindle and cell cycle
597 progression.[40] AURKA overexpression in breast cancer has been associated with
598 an ER-low/basal phenotype.[41] AURKA was previously implicated in mediating
599 endocrine resistance via SMAD-dependent downregulation of ER-alpha
600 expression.[42] Alisertib, an oral AURKA inhibitor, was well tolerated in HR+ MBC
601 patients when combined with fulvestrant, and anti-tumor activity was appreciated
602 in a phase I trial.[43] A randomized phase II study of this combination has
603 completed accrual (NCT02860000). We demonstrate that HR+ cells cultured to
604 resistance in CDK4/6i can demonstrate downregulation of RB1 or increased
605 expression of AURKA, both of which are associated with increased sensitivity to
606 LY3295668, a novel selective AURKA inhibitor. In screens to identify synthetic
607 lethal interactions with an RB1 mutation in lung and other cancers, the aurora
608 kinases emerged as key targets, and LY3295668 provoked tumor regression in
609 xenograft models of RB1-null small cell lung cancer.[34,44] We provide the first
610 evidence supporting AURKA as a mediator of resistance to CDK4/6i *in vitro* and
611 in tumor samples. Furthermore, in a patient with HR+ MBC who progressed after
612 a prolonged course of CDK4/6i-based therapy (analogous to our translational
613 culture-to-resistance experiment *in vitro*), subsequent treatment on a phase I trial
614 with LY3295668 was well tolerated and prompted prolonged clinical benefit. This
615 patient had high RB1 protein expression at the time of therapy initiation,
616 suggesting that her response was not governed by RB1 loss. Based upon these
617 translational insights, a phase I study exploring the utility of LY3295668 in

618 patients with HR+ MBC following progression on CDK4/6i was recently initiated
619 (NCT03955939).
620
621 Although one can consider targeting each individual resistance mechanism
622 directly, it may also be possible to target a smaller number of resistance "nodes"
623 or pathways upon which multiple resistance effectors converge. We previously
624 showed that *ERBB2* mutations and alterations in FGFR1/FGFR2 activate the
625 MAPK pathway in resistant HR+ MBC,[24,25] and MAPK pathway inhibition was
626 able to overcome this resistance. *RAS* mutations also activate the MAPK
627 pathway. The fact that multiple mechanisms of resistance to CDK4/6i activate the
628 MAPK pathway suggests that this may be an important node of resistance in
629 HR+ MBC – and that combining endocrine therapy and CDK4/6i with agents that
630 target MAPK such as MEK inhibitors, ERK inhibitors, and/or SHP2 inhibitors,
631 may be a unifying strategy to overcome or prevent resistance resulting from
632 multiple genetic aberrations. Similarly, both RB loss and AURKA amplification
633 are targetable with AURKA inhibitors. Taken together, it may be possible to
634 address all seven of these mechanisms (which account for at least 80% of the
635 resistant biopsies in this study) by targeting four nodes/pathways: AURKA,
636 MAPK, AKT/MTOR, and CCNE/CDK2 (Figure 6B).
637
638 We have identified multiple novel effectors of resistance to CDK4/6i in HR+
639 breast cancer, providing rationale to guide the development of a wide range of
640 precision-based clinical trials, in which patients with specific genomic or

641 molecular alterations are treated with novel therapeutic combinations designed to

642 circumvent or overcome resistance.

643 **Methods**

644 **Patients and Tumor Samples**

645 Prior to any study procedures, all patients provided written informed consent for
646 research biopsies and whole exome sequencing of tumor and normal DNA, as
647 approved by the Dana-Farber/Harvard Cancer Center Institutional Review Board
648 (DF/HCC Protocol 05-246). Metastatic core biopsies were obtained from patients
649 and samples were immediately snap frozen in OCT and stored in -80°C. Archival
650 FFPE blocks of primary tumor samples were also obtained. A blood sample was
651 obtained during the course of treatment, and whole blood was stored at -80°C
652 until DNA extraction from peripheral blood mononuclear cells (for germline DNA)
653 was performed. In a few instances, cell free DNA was obtained from plasma for
654 circulating tumor DNA analysis, as previously described.[49]

655

656 **Clinical Annotation and Biopsy Phenotypes**

657 Patient charts were reviewed to determine the sequence of treatments received
658 in the neoadjuvant, adjuvant, and metastatic setting as well as the temporal
659 relationship between available biopsy samples and CDK4/6i exposure.
660 Radiographic parameters were assigned via review of the imaging study
661 interpretations available in the patient record during the CDK4/6i treatment
662 course – tumors were defined as “responding” if any degree of tumor shrinkage
663 was reported by the evaluating radiologist, “stable” if there was felt to be no
664 meaningful change, “progressing” if lesions were increasing in size, or “mixed” if
665 comment was made denoting simultaneous shrinkage and growth in discordant

lesions. Tumors with a mixed response were excluded from analysis as a reliable phenotype could not be assigned. The "best radiographic response" (BRR) was then assigned as either "response" (R), "stable disease" (S), or "progression" (P) based upon the best radiographic parameter noted during the CDK4/6i treatment course.

Sensitive biopsies were defined as baseline samples obtained within 120 days prior to, or up to a maximum of 31 days after, CDK4/6i treatment initiation in a patient with subsequent clinical benefit (radiographic response or stable disease >6 months). Biopsies reflecting acquired resistance were obtained from patients who had experienced clinical benefit with CDK4/6i and had an available biopsy specimen either within 31 days of progression or at any time thereafter. Biopsies reflecting intrinsic resistance were obtained within 120 days prior to CDK4/6i initiation in patients without evidence of clinical benefit (defined as progression on the first interval restaging study or stable disease <6 months).

Whole Exome Sequencing

DNA was extracted from primary tumors, metastatic tumors, and peripheral blood mononuclear cells (for germline DNA) from all patients and whole exome sequencing was performed, as detailed below. In several instances, cell free DNA was obtained from plasma for circulating tumor DNA analysis, as previously described.[49]

688 ***DNA extraction****:* DNA extraction was performed as previously described.[50] For
689 whole blood, DNA is extracted using magnetic bead-based chemistry in
690 conjunction with the Chemagic MSM I instrument manufactured by Perkin Elmer.
691 Following red blood cell lysis, magnetic beads bind to the DNA and are removed
692 from solution using electromagnetized rods. Several wash steps follow to
693 eliminate cell debris and protein residue from DNA bound to the magnetic beads.
694 DNA is then eluted in TE buffer. For frozen tumor tissue, DNA and RNA are
695 extracted simultaneously from a single frozen tissue or cell pellet sample using
696 the AllPrep DNA/RNA kit (Qiagen). For FFPE tumor tissues, DNA and RNA are
697 extracted simultaneously using Qiagen's AllPrep DNA/RNA FFPE kit. All DNA is
698 quantified using Picogreen
699
700 ***Library Construction****:* DNA libraries for massively parallel sequencing were
701 generated as previously described[50] with the following modifications: the initial
702 genomic DNA input into the shearing step was reduced from 3µg to 10-100ng in
703 50µL of solution. For adapter ligation, Illumina paired-end adapters were
704 replaced with palindromic forked adapters (purchased from Integrated DNA
705 Technologies) with unique dual indexed 8 base index molecular barcode
706 sequences included in the adapter sequence to facilitate downstream pooling.
707 With the exception of the palindromic forked adapters, all reagents used for end
708 repair, A-base addition, adapter ligation, and library enrichment PCR were
709 purchased from KAPA Biosciences in 96-reaction kits. In addition, during the
710 post-enrichment solid phase reversible immobilization (SPRI) bead cleanup,

711 elution volume was reduced to 30µL to maximize library concentration, and a
712 vortexing step was added to maximize the amount of template eluted.
713
714 ***Solution-phase hybrid selection***: After library construction, hybridization and
715 capture were performed using the relevant components of Illumina's Rapid
716 Capture Exome Kit and following the manufacturer's suggested protocol, with the
717 following exceptions: first, all libraries within a library construction plate were
718 pooled prior to hybridization. Second, the Midi plate from Illumina's Rapid
719 Capture Exome kit was replaced with a skirted PCR plate to facilitate automation.
720 All hybridization and capture steps were automated on the Agilent Bravo liquid
721 handling system.
722
723 ***Preparation of libraries for cluster amplification and sequencing****:* After post-
724 capture enrichment, library pools were then quantified using quantitative PCR
725 (KAPA Biosystems) with probes specific to the ends of the adapters; this assay
726 was automated using Agilent's Bravo liquid handling platform. Based on qPCR
727 quantification, libraries were normalized and denatured using 0.1 N NaOH on the
728 Hamilton Starlet.
729
730 ***Cluster amplification and sequencing****:* Cluster amplification of denatured
731 templates was performed according to the manufacturer's protocol (Illumina)
732 using HiSeq 2500 Rapid Run v1/v2, HiSeq 2500 High Output v4 or HiSeq 4000
733 v1 cluster chemistry and HiSeq 2500 (Rapid or High Output) or HiSeq 4000

734 flowcells. Flowcells were sequenced on HiSeq 2500 using v1 (Rapid Run
735 flowcells) or v4 (High Output flowcells) Sequencing-by-Synthesis chemistry or v1
736 Sequencing-by-Synthesis chemistry for HiSeq 4000 flowcells. The flowcells were
737 then analyzed using RTA v.1.18.64 or later. Each pool of whole exome libraries
738 was run on paired 76np runs, with a two 8 base index sequencing reads to
739 identify molecular indices, across the number of lanes needed to meet coverage
740 for all libraries in the pool.
741
742 ***Sequence data processing****:* Exome sequence data processing was performed
743 using established analytical pipelines at the Broad Institute. A BAM file was
744 produced with the Picard pipeline (see URLs) which aligns the tumor and normal
745 sequences to the hg19 human genome build using Illumina sequencing reads.
746 The BAM was uploaded into the Firehose pipeline (see URLs), which manages
747 input and output files to be executed by GenePattern [51].
748
749 ***Sequencing quality control****:* Quality control modules within Firehose were
750 applied to all sequencing data for comparison of the origin for tumor and normal
751 genotypes and to assess fingerprinting concordance. Cross-contamination of
752 samples was estimated using ContEst.[52]
753
754 **Somatic Alteration Assessment**
755 MuTect[53] was applied to identify somatic single-nucleotide variants. Indelocator
756 (see URLs), Strelka[54], and MuTect2 (see URLs) were applied to identify small

757 insertions or deletions. A voting scheme with inferred indels requiring at least 2
758 out of 3 algorithms.
759
760 Artifacts introduced by DNA oxidation (so called OxoG) during sequencing were
761 computationally removed using a filter-based method.[55] In the analysis of primary
762 tumors that are formalin-fixed, paraffin-embedded samples [FFPE] we further
763 applied a filter to remove FFPE-related artifacts.[56]
764
765 Reads around mutated sites were realigned with Novoalign (see URLs) to filter
766 out false positive that are due to regions of low reliability in the reads alignment.
767 At the last step, we filtered mutations that are present in a comprehensive WES
768 panel of 8,334 normal samples (using the Agilent technology for WES capture)
769 aiming to filter either germline sites or recurrent artifactual sites. We further used
770 a smaller WES panel of normal 355 normal samples that are based on Illumina
771 technology for WES capture, and another panel of 140 normals sequenced within
772 our cohort[27] to further capture possible batch-specific artifacts. Annotation of
773 identified variants was done using Oncotator.[57]
774
775 **Copy Number and Copy Ratio Analysis**
776 To infer somatic copy number from WES, we used ReCapSeg (see URLs),
777 calculating proportional coverage for each target region (i.e., reads in the
778 target/total reads) followed by segment normalization using the median coverage

779 in a panel of normal samples. The resulting copy ratios were segmented using
780 the circular binary segmentation algorithm.[58]
781
782 To infer allele-specific copy ratios, we mapped all germline heterozygous sites in
783 the germline normal sample using GATK Haplotype Caller[59] and then evaluated
784 the read counts at the germline heterozygous sites in order to assess the copy
785 profile of each homologous chromosome. The allele-specific copy profiles were
786 segmented to produce allele specific copy ratios.
787
788 **Gene deletions and Bi-allelic inactivation**
789 For the inference of gene deletions and inactivations, as we aim to infer bi-allelic
790 inactivations (BiDel or “HOMDEL”), we take into account various mutational
791 events that may result in inactivation of both alleles. These mutational events
792 include: (1) loss of heterozygosity (LOH), (2) SNV (while excluding the following
793 variant classifications: "Silent", "Intron", "IGR", "5'UTR", "3'UTR", "5'Flank",
794 "3'Flank"), (3) short indels, (4) long deletions and gene rearrangements inferred
795 by SvABA,[60] and (5) potentially pathogenic germline events in cancer genes (see
796 description below).
797 Potentially pathogenic germline events: aiming to retain a subset of potentially
798 pathogenic germline events there are several features which are accounted for
799 including (1) ClinVar significant annotation among the following: Pathogenic.
800 Likely pathogenic, Conflicting interpretations of pathogenicity, risk factor or (2)
801 Variant Classification among the following: Splice_Site, Frame_Shift_Del,

802 Frame_Shift_Ins, Nonsense_Mutation. In addition (3) Genome Aggregation
803 Database (gnomAD)[61] less than 0.05 (indicating it is a rare variant)
804
805 **Cancer Cell Fraction and Evolutionary Analysis**
806 ***Analysis using ABSOLUTE***: To properly compare SNVs and indels in paired
807 metastatic and primary samples, we considered the union of all mutations called
808 in either of the two samples. We evaluated the reference and alternate reads in
809 each patient's primary and metastatic tumors, including mutations that were not
810 initially called in one of the samples. These mutations in matched samples were
811 used as input for ABSOLUTE.[62] The ABSOLUTE algorithm uses mutation-
812 specific variant allele fractions (VAF) together with the computed purity, ploidy,
813 and segment-specific allelic copy-ratio to compute cancer cell fractions (CCFs).
814
815 **Clonal structure and phylogenetic reconstruction of tumor evolution**
816 The clonal structure observed in individuals with more than a single tumor
817 sample was inferred with PyClone,[63] using the Beta Binomial model and the copy
818 number of each mutation inferred by ABSOLUTE with the parental copy number
819 parameter.
820 Subsequently, the inferred clonal structure was used to trace the evolutionary
821 history of the clones (phylogenic tree) using the ClonEvol,[64] retaining only clones
822 with at least four mutations and estimated cancer cellular fraction (cellular
823 prevalence) higher than 1%.
824

Evolutionary analysis of copy-number variation

Corrected quantification of copy number: gene amplifications are based on the purity corrected measure for the segment containing that gene, based on ABSOLUTE (rescaled_total_cn).[62] To better measure segment-specific copy-number, we subtracted the genome ploidy for each sample to compute copy number above ploidy (CNAP). CNAP of at least 3 are considered as amplifications ("AMP"), CNAP above 1.5, but below 3 are considered low amplification ("GAIN"), and are not depicted in our mutational landscape (Figure 1). CNAP of at least 6 are considered high amplifications ("HighAMP"), and CNAP of at least 9 and no more than 100 genes[65] is considered very high focal amplification ("FocalAMP").

The evolutionary classification of amplifications accounts for the magnitude of the observed copy-number difference between the pre-treatment and the post-treatment samples. If the difference between the CNAP of the post-treatment and the CNAP of the pre-treatment is smaller than 50%, the amplification is defined as "Shared". If the CNAP of the post-treatment is larger than the CNAP by more than 50% and the lower pre-treatment CNAP is not at "FocalAMP" level, the evolutionary classification is "Acquired". If CNAP of the post-treatment is smaller by at least 50%, comparing to the pre-treatment sample and the lower post-treatment CNAP is not at "FocalAMP" level, the evolutionary classification is "Loss". Otherwise, the evolutionary classification of amplifications is defined as "Indeterminate".

Cell Culture

HR+/HER2- human breast cancer cell lines T47D (HT-133) and MCF7 (HTB-22) were obtained from American Type Culture Collection (ATCC). T47D and MCF7 cells were cultured in RPMI 1640 medium (no phenol red; Gibco, 11835-030) and MEMα (nucleosides, no phenol red; Gibco, 41061029) respectively, both supplemented with 10% fetal bovine serum (Gemini bio-products, 100-106) and 1% penicillin-streptomycin-glutamine. HEK 293T/17 (CRL-11268) were obtained from ATCC and cultured in DMEM (high glucose, pyruvate; Gibco, 11995065), supplemented with 10% fetal bovine serum (Gemini bio-products, 100-106) and 1% penicillin-streptomycin-glutamine (Gibco, 10378016).

Candidate driver plasmid and cell line production

AKT1 (BRDN0000464992), KRASG12D (BRDN0000553331), AURKA (TRCN0000492002), CCNE2 (ccsbBroadEn_11340), and GFP bacterial streaks were obtained from the Genetic Perturbation Platform, Broad Institute, MA. RB1 and CRISPR non-targeting guide cells were obtained as a gift Flora Luo and the Garraway laboratory. The CCNE2 construct was cloned into a pLX307 vector using the LR reaction kit (Life Technologies, 11791019). All construct plasmids were prepared using the Plasmid Plus Midi Kit (Qiagen, 12943). To generate lentivirus for each construct, 293T cells were transfected with Opti-MEM (Gibco, 31985-062), FuGENE HD (Promega, E2311), VSV-G envelope plasmid, and □8.91 packaging plasmid. After 72h of incubation, supernatant was filtered through a 0.45 µL filter (Corning, 431225) and lentivirus presence was tested

using Lenti-X GoStix (TakaraBio, 631244). 500µL – 1mL of virus was added to a 60-mm dish containing T47D (or MCF7) cells and medium with 4µg/mL of polybrene (Millipore Sigma, TR-1003-G). After overnight incubation, cells were moved to a 100-mm dish and again incubated overnight. The medium was replaced and 0.5µg/mL of puromycin (Gibco, A1113803) were added to KRASG12D, AURKA, CCNE2, RB1 and CRISPR constructs, and 6-10µg/mL of blasticidin (Gibco, A1113903) were added to GFP and AKT1 constructs. Plates were compared to uninfected control plates, and after 2 days of selection, were plated for drug sensitivity assay and harvested for western blotting as described below.

Kill Curves/Drug Sensitivity Assay

Cells were plated at a density of 1000 cells/well in RPMI and 1500 cells/well in MEMα, for T47D and MCF7, respectively, in 96 well plates (PerkinElmer, 6005181). The experiments were plated in triplicate, for ten doses of the drug of interest. Palbociclib doses ranging from 1 nM to 10 µM were prepared from a 10 mM stock solution in molecular biology grade water (Corning, 46-000-CI); abemaciclib doses ranging from 1 nM to 10 µM were prepared from a 10 mM stock solution in molecular biology grade water (Corning, 46-000-CI); fulvestrant doses ranging from 0.01 nM to 1 µM were prepared from a 20 mM stock solution in DMSO (Sigma-Aldrich, D2650). The next day, cells were treated with the range of doses of the drug of interest. Cells were re-treated three days later. After treatment has been applied for eight days, the 96-well plates were brought

894 out of the incubator and allowed to equilibrate to room temperature. The medium
895 was replaced with 50 µL of fresh medium per well. 50 µL of CellTiter-Glo 2.0
896 (Promega, G9241) was added to each well, the plate was shaken at 200 rpm for
897 2 min, and then allowed to equilibrate at room temperature for fifteen minutes as
898 per the CellTiter-Glo 2.0 Assay Technical Manual. Average background
899 luminesce reading was calculated from plate wells containing only medium, and
900 was subtracted from all values. The values were then averaged for each triplicate
901 and standard deviations were calculated. The data were normalized to the no-
902 drug, vehicle control for each construct. The calculated averages and standard
903 deviations were visualized on GraphPad Prism 7 using the log(inhibitor) vs.
904 response (three parameters) preset protocol.
905
906 **Chemicals and antibodies**
907 Chemicals utilized included palbociclib (Selleck Chemicals, S1116), abemaciclib
908 (ApexBio, A1794), and fulvestrant (Sigma-Aldrich, I4409). Primary antibodies
909 utilized included antibodies against β-Actin (Santa Cruz, sc-47778), Rb (Cell
910 Signaling Technology, clone 4H1, 9309), Akt (CST, 9272), Ras (CST, clone
911 D2C1, 8955), Aurora A (CST, clone D3E4Q, 14475), and Cyclin E2 (CST, 4132),
912 in addition to the secondary antibodies goat anti-rabbit (Invitrogen, 32260) and
913 goat anti-mouse (Invitrogen, A16090).
914

915 **Western blotting**

916 A near-confluent T75 (~7x10^6 cells) was spun down and the pellet kept at -20C.
917 The pellet was then lysed in 1mL of lysis buffer consisting of RIPA buffer (Sigma-
918 Aldrich, R0278), dithiothreitol (DTT, Invitrogen, 15508013), phenylmethane
919 sulfonyl fluoride (PMSF, Sigma-Aldrich, P7626), and PhosStop (Sigma-Aldrich,
920 4906837001). Lysate was rotated at 15 r.p.m for 15 minutes at 4°C, then
921 centrifuged at 14,000g for 15 minutes at 4°C, preserving the supernatant. Protein
922 concentration was quantified via bicinchoninic acid assay (Pierce BCA Protein
923 Assay Kit, Thermo Fisher Scientific, 23225) and Tecan i-control software pre-set
924 BCA program. Samples were prepared using 40µg of protein, Bolt LDS Sample
925 Buffer (Invitrogen, B0007), and DTT and heated to 95°C for 5 min. The samples
926 were run on a Bolt 4-12% Bis-Tris Plus Gel (Invitrogen, NW04120BOX) in 1X
927 Bolt MOPS SDS Running Buffer (Invitrogen, B000102) for 1hr at 130V. Protein
928 was transferred to nitrocellulose membranes via the Trans-Blot Turbo Transfer
929 System (Bio-Rad, 1704150) following the turbo mini preset protocol (1.3A 25V
930 7Min) two times. Membranes were blocked in 5% milk in Tris-buffered saline
931 (Bio-Rad, 1706435) with 0.1% Tween-20 (Sigma-Aldrich, P9416) for one hour at
932 room temperature. Membranes were incubated overnight at 4°C with primary
933 antibodies that were diluted 1:1000 (with the exception of Rb, which was diluted
934 1:500) in 5% milk in TBS-T. After incubation, membranes were washed 3 times
935 for 10min with 1X TBS-T and incubated with secondary antibody diluted 1:2000
936 in 5% milk in TBS-T for 1h at room temperature. Membranes were then washed
937 3 times for 10min with 1X TBS-T. After washing, membranes were treated with

938 Pierce ECL Plus Western Blotting Substrate (Thermo Fisher Scientific, 32132) for
939 5 minutes and exposed to autoradiography film (Denville, 1159M38).
940
941 For resistant/derivative cell lines: cells were washed with PBS and lysed in lysis
942 buffer (1% triton X-100, 25mM Tris pH 7.5, 150mM NaCl, 1mM EDTA, Halt
943 Protease/phosphatase inhibitor cocktail), and protein concentration was
944 assessed by BCA protein assay (Pierce 23225). Equal amounts of protein were
945 electrophoresed on 4-20% BioRad Tris Glycine Gels (BioRad 5671094)
946 transferred to nitrocellulose (BioRad 1704159) and probed with primary
947 antibodies. Antibodies were purchased from Cell Signaling Technology for Rb
948 Total (9307), pRb S780 (3590), pRb S807/811 (8516), CCNE2 (4132), Akt S473
949 (4051), S6 total (2317), S6 S240/244 (4838), ERK total (3042), pERK T202/Y204
950 (4370, 4376) and R&D Systems AurA (AF3295). Digiwest® protein profiling of
951 MDA-MB-361-AR was also conducted with NMI TT.
952
953
954 **Resistant cell line generation**
955 The methods for generating resistant cell lines were described previously.[34]
956 Briefly, MDA-MB-361, T47D and MCF-7 ER+ breast cancer cell lines were used
957 to derive variants with acquired resistance to abemaciclib or palbociclib. T47D
958 (HTB-133), MCF-7 (HTB-22) and MDA-MB-361 (HTB-27) were purchased from
959 The American Type Culture Collection (ATCC). Cell lines were cultured in RPMI-
960 1640 medium (Gibco 22400-089) + 10% FBS (Hyclone SH30071.03), Eagles

961 Essential Medium (Gibco 11090-081) + 10% FBS and Liebovitz L-15 Medium
962 (Gibco 11215-064) + 20% FBS, respectively. Resistant cell lines were generated
963 by chronic treatment with either abemaciclib or palbociclib alone or in
964 combination with fulvestrant. Cell cultures were initiated in low doses of
965 compound approximating the IC50 until cells grew to 80% confluence. Cells were
966 then passaged and treated with incrementally higher doses. This process was
967 repeated several times until cells were able to grow in the presence of drugs at
968 clinically meaningful concentrations. Once resistant cell lines were established,
969 the stability of resistance was assessed with a 21 day dosing holiday. Resistance
970 remained stable in all cell lines except for T47D-AR and T47D-PR which became
971 almost completely resensitized to the CDK4/6i after the 21 day drug-free period.
972 All resistant derivatives resistant were found to be cross resistant to the CDk4/6i
973 that was not used in the selection step. Short tandem repeat (STR) analysis was
974 performed to verify the authenticity of the cell lines.
975

976 **Proliferation Assays**

977 Cells were plated onto poly-D-lycine plates (Corning 354640) and treated in
978 replicate with a dose curve of compounds of interest. Cells were allowed to grow
979 for two doubling times and proliferation was measured by CellTiter-Glo®
980 (Promega G7571) or CyQuant (Invitrogen C3511) per manufacturer's protocol.
981 Data analysis was carried out using Prism software.
982

983 **LY3295668 Phase 1/2 Clinical Trial**

The patient vignette provided in this manuscript was shared from an ongoing phase 1/2 study. Please see protocol NCT03092934 at www.clinicaltrials.gov for details related to the study location, eligibility, and compound. This is an open-label, multicenter study of patients with locally advanced or metastatic solid tumors and disease progression after 1-□4 prior treatment regimens. The phase 1 portion of the protocol is designed to evaluate the primary objective of determining the maximum tolerated dose (MTD); secondary objectives included evaluation of tolerability and overall safety profile of LY3295668. The primary objective of the phase 2 study portion is to evaluate the objective response rate of tumors after treatment with LY3295668. Patients in the phase 2 study were required to have estrogen receptor and/or progesterone receptor positive, human epidermal growth factor receptor 2 (HER2) negative, breast cancer with prior exposure to and progression on on a hormone therapy and a CDK4/6 inhibitor.

Acknowledgements

We thank Laura Dellostritto, Lori Marini, Nelly Oliver, Shreevidya Periyasamy, Janet Files, Sara Hoffman, and Colin Mackichan for assistance with patient sample collection and annotation. We are grateful to all the patients who volunteered for our tumor biopsy protocol and generously provided the tissue analyzed in this study.

Grant support

This work was supported by the Department of Defense W81XWH-13-1-0032 (NW), AACR Landon Foundation 13-60-27-WAGL (NW), NCI Breast Cancer SPORE at DF/HCC #P50CA168504 (NW, NUL and EPW), Susan G. Komen CCR15333343 (NW), The V Foundation (NW), The Breast Cancer Alliance (NW), The Cancer Couch Foundation (NW), Twisted Pink (NW), Hope Scarves (NW), Breast Cancer Research Foundation (NUL and EPW), ACT NOW (to Dana-Farber Cancer Institute Breast Oncology Program), Fashion Footwear Association of New York (to Dana-Farber Cancer Institute Breast Oncology Program), Friends of Dana-Farber Cancer Institute (to NUL), National Comprehensive Cancer Network/Pfizer Independent Grant for Learning & Change (to NUL), the Dana-Farber Cancer Institute T32 (to SAW), Wong Family Translational Research Award (to SAW), and the Conquer Cancer Foundation/Twisted Pink/American Society of Clinical Oncology Young Investigator Award (to SAW).

Figure Legends

Figure 1. The genomic landscape of CDK4/6i resistance is heterogeneous, with multiple potential driver events.

(a) Biopsy phenotypes were assigned as *sensitive, acquired resistance,* or *intrinsic resistance* based upon timing of the biopsy relative to CDK4/6i exposure (d - days), best radiographic response (BRR), and duration of treatment. Patients were categorized as experiencing clinical benefit on CDK4/6i if interval restaging demonstrated a response or disease stability for at least six months. (b) Mutational matrix (CoMut) depicting the genomic landscape of the CDK4/6i cohort (n = 59 biopsies, 58 patients). Copy number alterations and mutational events in select genes of interest are shown. Clinical parameters (shown at the top) include receptor status, anti-estrogen agent, CDK4/6 inhibitor, best radiographic response (P – progression, R – response, S – stable), biopsy phenotype (S – sensitive, IR – intrinsic resistance, AR – acquired resistance), treatment duration (days), biopsy timing relative to treatment initiation (days), time since metastatic diagnosis (days), and number of lines of prior treatment. (c) Phenotype distribution plot demonstrating a higher frequency of copy number amplifications in Aurora Kinase A (AURKA) among resistant biopsies (AR + IR, left) compared to sensitive biopsies (right, 0.0081, Welch test). (d) Bar plot visualization of mutational (M) and/or copy number alterations (A – amplification, LA – low amplification) in select genes. The proportional enrichment (fraction of samples demonstrating alteration) in sensitive biopsies (left, blue) and resistant biopsies (AR + IR, right, red) is included.

Figure 2. Acquired resistance to CDK4/6i in patients with pre-treatment and post-progression biopsies demonstrates convergent evolution of biallelic RB1 disruption and evolved AKT1 activation.

Phylogenetic analysis depicting the evolutionary history for seven patients with acquired alterations, with clonal evolutionary dynamics demonstrating: (a) acquired polyclonal ESR1 mutations after aromatase inhibition, followed by convergent evolution of RB1 inactivation, with different RB1-inactivating mutations acquired in two parallel sibling clones; (b) Acquired AKT1 amplification; (c) No notable candidate for acquired mechanism of resistance (MOR); (d) Acquired AKT1 (W80R) mutation; (e) No notable candidate for acquired MOR; (f) Acquired inactivation of DNA Mismatch Repair Protein (MLH3); and (g) Acquired activating ESR1 mutation (Y537S) and amplification in AKT3.

Figure 3. Clinical vignettes for candidate resistance drivers in representative patients (RB1, AKT1, RAS, and CCNE2).

Clinical vignettes including treatment sequence, timing of metastatic progression, and available biopsies with key genomic findings are provided for the following - (a) four patients with biallelic alterations in RB1, including a patient with multiple biopsies and convergent evolution toward RB1 disruption (top, phylogenetic analysis for this patient is provided in Figure 2A). (b) Three patients with acquired alterations in AKT1 following progression on CDK4/6i. In the first (top), a new

mutation in AKT1 W80R was identified. In the second (middle), a baseline alteration (AKT1 L52H) was identified at the time of diagnosis; at the time of progression on CDK4/6i, two biopsies were obtained – both demonstrating the baseline AKT1 L52H mutation, one also demonstrating an acquired amplification of the wild-type AKT1 protein (phylogenetic analyses for these patients are provided in Figure 2B and D). (c) Three patients with resistance to CDK4/6i and RAS-family alterations (including two instances of KRAS G12D and one instance of HRAS mutation). (d) Three patients with intrinsic resistance to CDK4/6i and amplification events in CCNE2.

Figure 4. Candidate genomic alterations provoke CDK4/6i resistance *in vitro*.

(a) T47D cells were modified via CRISPR-mediated downregulation (RB1) or lentiviral overexpression (AKT1, KRAS G12D, AURKA, CCNE2) to interrogate potential resistance mediators identified in patient biopsy samples. Western blotting with the indicated antibodies is included. (b-f) Modified T47D cells were exposed to escalating doses of CDK4/6i (palbociclib – left, abemaciclib – right) and viability was estimated via cell-titer-glo (CTG) assay. Control (CRISPR non-targeting guide or GFP) cells are plotted along with the resistance driver of interest (RB1 – b, AKT1 – c, KRAS G12D – d, AURKA – e, CCNE2 – f). Parental and variant cell lines are normalized to vehicle control and viability is plotted as a function of increasing CDK4/6i (graphed as triplicate average +/- standard deviation). All variants provoke CDK4/6i resistance (to both palbociclib and

abemaciclib) *in vitro* in T47D cells. Corresponding IC50 values are included in Supplemental Table 7.

Figure 5. Candidate mutations emerge in cell lines cultured under CDK4/6i selective pressure and define new therapeutic dependencies *in vitro.*

(a) Breast cancer cell lines (T47D, MCF7, MDA-MB-361) were cultured long-term to resistance in the presence of CDK4/6i (palbociclib, abemaciclib). The resulting cell lines which emerged were subjected to western blotting for putative mediators of drug resistance (RB1, AKT1, KRAS/ERK, AURKA, and CCNE2). (b-c) T47D cells cultured to resistance in the presence of abemaciclib demonstrated low levels of RB1 expression (T47D-AR1) and increased sensitivity to the AURKA inhibitor LY3295668. MDA-MB-361 cells cultured to resistance in the presence of abemaciclib demonstrated high levels of ERK activation (361-AR1) and increased sensitivity to the ERK inhibitor LY3214996. MDA-MB-361 cells cultured to resistance in the presence of palbociclib demonstrated high levels of AURKA (361-PR1) and increased sensitivity to the AURKA inhibitor LY3295668. MCF7 cells cultures to resistance in the presence of palbociclib demonstrated increased levels of CCNE2 (MCF7-PR1) and increased sensitivity to the CHEK1 inhibitor prexasertib.

Figure 6. A novel aurora kinase A inhibitor demonstrates therapeutic efficacy in a patient with metastatic HR+ breast cancer after progression on CDK4/6i.

(a) A patient with locally advanced HR+/HER2- breast cancer developed metastatic recurrence on adjuvant tamoxifen. She received CDK4/6i and letrozole in the first line setting with prolonged clinical benefit (>3 years). At progression, she was placed on trial with the AURKA inhibitor LY3295668; she subsequently experienced prolonged disease control ~11 months. Baseline staging studies following progression on CDK4/6i in the patient described are included (top); she had osseous metastatic disease and visceral disease limited to the foci noted in the liver. Two interval restaging studies (top) demonstrate disease stability/mild response. Liver biopsy obtained at the time of progression on CDK4/6i and prior to LY3295668 demonstrated high Ki67 and high RB1 protein expression via immunohistochemistry (IHC, 10x) (bottom). (b) Schematic diagram demonstrating the potential utility of next-generation sequencing following progression on CDK4/6i; actionable alterations in RB1, ERBB2, FGFR2, AKT1, RAS, AURKA, and CCNE2 could dictate informed selection of targeted therapies as indicated.

Supplementary Figure Legends

Supplemental Figure 1. Subgroup genomic analysis of the CDK4/6i cohort based upon anti-estrogen exposure.

Heatmaps demonstrating key genomic events (both copy number alteration and mutation) in a subset of genes for (a) patients with exposure to CDK4/6i and aromatase inhibitor (AI) and for (b) patients with exposure to CDK4/6i and fulvestrant. The gene set and clinical parameters are identical to those provided in Figure 1B.

Supplemental Figure 2. Higher AURKA expression observed even in low-amplification tumors in TCGA

Breast tumor from the TCGA dataset were stratified based on the genomic AURKA copy number (low amplification – left, no amplification – right; high amplification excluded) and plotted against AURKA RNA expression. Higher AURKA RNA expression was observed in low AURKA-amplification compared to non-amplified tumors in these TCGA samples.

Supplemental Figure 3. Candidate resistance mutations in representative patients – key counterexamples.

Biopsies demonstrating CDK4/6i sensitivity despite the presence of putative resistance drivers were identified and clinical vignettes were generated. (a) A

patient with bone-only metastatic progression was placed on first-line CDK4/6i and letrozole. A canonical AKT1 E17K alteration was identified at the time of metastatic progression. This patient has had stable osseous metastatic disease on interval repeat imaging and remained on treatment at the time of data cutoff. (b) A patient with de novo metastatic HR+/HER2- breast cancer was treated with tamoxifen and subsequently received palbociclib and letrozole. Prior to CDK4/6i exposure, which lasted for a duration exceeding one year, a baseline low-level amplification in CCNE2 was identified. (c) A patient was diagnosed with localized HR-/HER2+ breast cancer and treated with chemotherapy. Late metastatic relapse occurred with a new contralateral tumor, now HR+/HER2-. Following progression on tamoxifen, and prior to treatment with CDK4/6i and letrozole, an ERBB2 mutation was identified. Despite the presence of this alteration, the patient has had a durable ongoing response to CDK4/6i-based treatment.

Supplemental Figure 4. Candidate alterations provoke CDK4/6i resistance *in vitro* (MCF7).

(a) MCF7 cells were modified via CRISPR-mediated downregulation (RB1) or lentiviral overexpression (AKT1, KRAS G12D, AURKA, CCNE2) to interrogate potential resistance mediators identified in patient biopsy samples. Western blotting with the indicated antibodies is included. (b-f) Modified MCF7 cells were exposed to escalating doses of CDK4/6i (palbociclib – left, abemaciclib – right) and viability was estimated via cell-titer-glo (CTG) assay. Control (CRISPR non-targeting guide, GFP) cells are plotted along with the resistance driver of interest

(RB1 – b, AKT1 – c, KRAS G12D – d, AURKA – e, CCNE2 – f). Parental and variant cell lines are normalized to vehicle control and viability is plotted as a function of increasing CDK4/6i (graphed as triplicate average +/- standard deviation). RB1, AKT1, and CCNE2 provoke CDK4/6i resistance (to both palbociclib and abemaciclib) *in vitro* in MCF7 cells. Corresponding IC50 values are included in Supplemental Table 7.

Supplemental Figure 5. Candidate alterations provoke variable anti-estrogen resistance *in vitro*.

Cell lines modified to reflect potential resistance drivers (per Figure 4 and Supplemental Figure 6; T47D – left, MCF7 - right) were exposed to escalating doses of fulvestrant (a – e). Drug response was assessed via cell-titer-glo (CTG) assay. Control (CRISPR non-targeting guide, GFP) cells are plotted along with the resistance driver of interest (RB1 – a, AKT1 – b, KRAS G12D – c, AURKA – d, CCNE2 – e). Parental and variant cell lines are normalized to vehicle control and viability is plotted as a function of increasing CDK4/6i (graphed as triplicate average +/- standard deviation). AKT1 and CCNE2 provoke fulvestrant resistance *in vitro* in both T47D and MCF7 cells. RB1 provokes minimal fulvestrant resistance in both T47D and MCF7. KRAS G12D and AURKA provoke significant fulvestrant resistance in T47D; KRAS G12D provokes minimal resistance in MCF7, while AURKA does not convey any resistance in MCF7. Corresponding IC50 values are included in Supplemental Table 7.

Supplemental Figure 6. MDA-MB-361-AR-1 demonstrates upregulation of RAS-ERK pathway effectors via proteomic analysis.

Digiwest proteomic analysis of MDA-MB-361-AR-1 cells versus parental MCF-7 cells demonstrates increased activation of multiple RAS-pathway effectors including KRAS, MEK, and ERK. These results suggest that the upregulation in pERK noted via western blot analysis correlates with pathway activation in the derivative cells.

Supplementary Table Legends

Supplemental Table 1. Clinical samples included in landscape analysis (excel file, 1 tab)

Clinical information including treatment regimen, treatment duration (days), best radiographic response (BRR), and timing of the biopsy relative to treatment initiation/cessation (days). Biopsy sample information including receptor status, biopsy site, cancer-purity of sample and treatment-related information

Supplemental Table 2. Clinical cohort characteristics (excel file, 1 tab)

Clinical parameters of interest are included at the patient level (n = 58).

Supplemental Table 3. Exome and mutational information (excel file, 3 tabs)

Tab 1 – Exome-wide single nucleotide variants (SNVs) and Indels; Tab 2- Copy Number Variants (CNVs) at the segment level including Copy Number Above Ploidy (CNAP); Tab 3 - CNVs and Bi-Allelic inactivation at the single-gene level among oncogene and tumor suppressor gene candidates; Tab 4 – Genomic alterations among candidate mechanisms of resistance (MOR) among the resistance samples in our cohort. Candidate MOR genes include – RB1 with HOMDEL mutation type, AURKA - with Amplifications including GAIN) CCNE2 AKT1, RAS (KRAS, NRAS, and HRAS), ERBB2, and FGFR (FGFR1, FGFR2, and FGF3) – with activating evens – Amplifications and putative activating SNVs;

Tab 5 – literature based list of known oncogenes (n=489) and tumor suppressor gene candidates (n=483).[45-48]

Supplemental Table 4. Enrichment analysis of mutation in resistant vs. sensitive tumors (excel file, 1 tab)

Fisher's Exact test (single-side, for enrichment) comparing gene-specific the frequency of mutational events: HOMDEL==Bi-Allelic inactivation (among tumor suppressor candidates), IHC loss (for ER receptor), and gene activation by copy-number amplification – GAIN.up== CNAP>=1.5, AMP.up== CNAP>=3, or gene activation by either amplification or activating mutation – ACT==CNAP>=3 or Gain-of-function or recurring mutation, ACT.inc== same as ACT, but including non-recurring missense mutation (among oncogene candidates)

Supplemental Table 5. Driver enrichment within patient populations (excel file, 1 tab)

Sensitive, intrinsic resistant, and acquired resistant biopsies harboring any of the 8 potential driver alterations are quantified and graphed in figure 1D. Potential driver alterations include ER loss, amplification/mutation of ERBB2, FGFR2, CCNE2, AURKA, RAS, AKT1 and biallelic disruption of RB1.

Supplemental Table 6. Evolutionary analysis and clonal fraction across 7 patients with multiple biopsies spanning pre- and post-treatment timepoints (excel file, 7 tabs)

For each of the 7 patients with multiple biopsies, the clonal prevalence and evolutionary dynamic information is provided by depicting for each SNV (mutation_id) the cancer-cell fraction (cellular_prevalence) in each of the samples/time-point (sample_id), among other clone/cluster related information

Supplemental Table 7. - IC50 Values for Drug Treatment Assays

Corresponding IC50 estimates to the various drug response relationships provide in Figure 4 and Supplemental Figures 4 and 5 are provided here

Supplemental Table 8. - IC50 Values for Culture to Resistance Experiments

Corresponding IC50 estimates to the various drug response relationships provided in Figure 5 are provided here

References

1. Spring, L.M., Wander, S.A., Zangardi, M. & Bardia, A. CDK 4/6 Inhibitors in Breast Cancer: Current Controversies and Future Directions. *Curr Oncol Rep* **21**, 25 (2019).
2. Ballinger, T.J., Meier, J.B. & Jansen, V.M. Current Landscape of Targeted Therapies for Hormone-Receptor Positive, HER2 Negative Metastatic Breast Cancer. *Front Oncol* **8**, 308 (2018).
3. Finn, R.S.*, et al.* Palbociclib and Letrozole in Advanced Breast Cancer. *N Engl J Med* **375**, 1925-1936 (2016).
4. Cristofanilli, M.*, et al.* Fulvestrant plus palbociclib versus fulvestrant plus placebo for treatment of hormone-receptor-positive, HER2-negative metastatic breast cancer that progressed on previous endocrine therapy (PALOMA-3): final analysis of the multicentre, double-blind, phase 3 randomised controlled trial. *Lancet Oncol* **17**, 425-439 (2016).
5. Hortobagyi, G.N.*, et al.* Ribociclib as First-Line Therapy for HR-Positive, Advanced Breast Cancer. *N Engl J Med* **375**, 1738-1748 (2016).
6. Goetz, M.P.*, et al.* MONARCH 3: Abemaciclib As Initial Therapy for Advanced Breast Cancer. *J Clin Oncol* **35**, 3638-3646 (2017).
7. Sledge, G.W., Jr.*, et al.* MONARCH 2: Abemaciclib in Combination With Fulvestrant in Women With HR+/HER2- Advanced Breast Cancer Who Had Progressed While Receiving Endocrine Therapy. *J Clin Oncol* **35**, 2875-2884 (2017).

8. Sledge, G.W., Jr., *et al.* The Effect of Abemaciclib Plus Fulvestrant on Overall Survival in Hormone Receptor-Positive, ERBB2-Negative Breast Cancer That Progressed on Endocrine Therapy-MONARCH 2: A Randomized Clinical Trial. *JAMA Oncol* (2019).

9. Im, S.A., *et al.* Overall Survival with Ribociclib plus Endocrine Therapy in Breast Cancer. *N Engl J Med* **381**, 307-316 (2019).

10. Dickler, M.N., *et al.* MONARCH 1, A Phase II Study of Abemaciclib, a CDK4 and CDK6 Inhibitor, as a Single Agent, in Patients with Refractory HR(+)/HER2(-) Metastatic Breast Cancer. *Clin Cancer Res* **23**, 5218-5224 (2017).

11. Finn, R.S., *et al.* PD 0332991, a selective cyclin D kinase 4/6 inhibitor, preferentially inhibits proliferation of luminal estrogen receptor-positive human breast cancer cell lines in vitro. *Breast Cancer Res* **11**, R77 (2009).

12. Herrera-Abreu, M.T., *et al.* Early Adaptation and Acquired Resistance to CDK4/6 Inhibition in Estrogen Receptor-Positive Breast Cancer. *Cancer Res* **76**, 2301-2313 (2016).

13. Condorelli, R., *et al.* Polyclonal RB1 mutations and acquired resistance to CDK 4/6 inhibitors in patients with metastatic breast cancer. *Ann Oncol* **29**, 640-645 (2018).

14. O'Leary, B., *et al.* The Genetic Landscape and Clonal Evolution of Breast Cancer Resistance to Palbociclib plus Fulvestrant in the PALOMA-3 Trial. *Cancer Discov* **8**, 1390-1403 (2018).

15. Fribbens, C., *et al.* Plasma ESR1 Mutations and the Treatment of Estrogen Receptor-Positive Advanced Breast Cancer. *J Clin Oncol* **34**, 2961-2968 (2016).

16. Tolaney, S.M., *et al.* Abstract 4458: Clinical significance of PIK3CA and ESR1 mutations in ctDNA and FFPE samples from the MONARCH 2 study of abemaciclib plus fulvestrant. *Cancer Research* **79**, 4458-4458 (2019).

17. Costa, C., *et al.* PTEN loss mediates clinical cross-resistance to CDK4/6 and PI3Kalpha inhibitors in breast cancer. *Cancer Discov* (2019).

18. Jansen, V.M., *et al.* Kinome-Wide RNA Interference Screen Reveals a Role for PDK1 in Acquired Resistance to CDK4/6 Inhibition in ER-Positive Breast Cancer. *Cancer Res* **77**, 2488-2499 (2017).

19. Yang, C., *et al.* Acquired CDK6 amplification promotes breast cancer resistance to CDK4/6 inhibitors and loss of ER signaling and dependence. *Oncogene* **36**, 2255-2264 (2017).

20. Caldon, C.E., *et al.* Cyclin E2 overexpression is associated with endocrine resistance but not insensitivity to CDK2 inhibition in human breast cancer cells. *Mol Cancer Ther* **11**, 1488-1499 (2012).

21. Turner, N.C., *et al.* Cyclin E1 Expression and Palbociclib Efficacy in Previously Treated Hormone Receptor-Positive Metastatic Breast Cancer. *J Clin Oncol*, JCO1800925 (2019).

1328 22. Li, Z.*, et al.* Loss of the FAT1 Tumor Suppressor Promotes Resistance to
1329 CDK4/6 Inhibitors via the Hippo Pathway. *Cancer Cell* **34**, 893-905 e898
1330 (2018).
1331 23. Cornell, L., Wander, S.A., Visal, T., Wagle, N. & Shapiro, G.I. MicroRNA-
1332 Mediated Suppression of the TGF-beta Pathway Confers Transmissible
1333 and Reversible CDK4/6 Inhibitor Resistance. *Cell Rep* **26**, 2667-2680
1334 e2667 (2019).
1335 24. Mao, P.*, et al.* Acquired FGFR and FGF alterations confer resistance to
1336 estrogen receptor (ER) targeted therapy in ER+ metastatic breast cancer.
1337 *bioRxiv*, 605436 (2019).
1338 25. Nayar, U.*, et al.* Acquired HER2 mutations in ER(+) metastatic breast
1339 cancer confer resistance to estrogen receptor-directed therapies. *Nat*
1340 *Genet* **51**, 207-216 (2019).
1341 26. Formisano, L.*, et al.* Aberrant FGFR signaling mediates resistance to
1342 CDK4/6 inhibitors in ER+ breast cancer. *Nat Commun* **10**, 1373 (2019).
1343 27. Cohen, O.*, et al.* Abstract S1-01: Whole exome and transcriptome
1344 sequencing of resistant ER+ metastatic breast cancer. *Cancer Research*
1345 **77**, S1-01-S01-01 (2017).
1346 28. Abba, M.C.*, et al.* A Molecular Portrait of High-Grade Ductal Carcinoma In
1347 Situ. *Cancer Res* **75**, 3980-3990 (2015).
1348 29. Zehir, A.*, et al.* Mutational landscape of metastatic cancer revealed from
1349 prospective clinical sequencing of 10,000 patients. *Nat Med* **23**, 703-713
1350 (2017).

30. Jeselsohn, R., Buchwalter, G., De Angelis, C., Brown, M. & Schiff, R. ESR1 mutations-a mechanism for acquired endocrine resistance in breast cancer. *Nat Rev Clin Oncol* **12**, 573-583 (2015).

31. Tate, J.G.*, et al.* COSMIC: the Catalogue Of Somatic Mutations In Cancer. *Nucleic Acids Res* **47**, D941-D947 (2019).

32. Marchio, C.*, et al.* The genetic landscape of breast carcinomas with neuroendocrine differentiation. *J Pathol* **241**, 405-419 (2017).

33. Bessiere, L.*, et al.* A Hot-spot of In-frame Duplications Activates the Oncoprotein AKT1 in Juvenile Granulosa Cell Tumors. *EBioMedicine* **2**, 421-431 (2015).

34. Gong, X.*, et al.* Aurora A Kinase Inhibition Is Synthetic Lethal with Loss of the RB1 Tumor Suppressor Gene. *Cancer Discov* **9**, 248-263 (2019).

35. Etemadmoghadam, D.*, et al.* Synthetic lethality between CCNE1 amplification and loss of BRCA1. *Proc Natl Acad Sci U S A* **110**, 19489-19494 (2013).

36. Drago, J.Z.*, et al.* FGFR1 gene amplification mediates endocrine resistance but retains TORC sensitivity in metastatic hormone receptor positive (HR+) breast cancer. *Clin Cancer Res* (2019).

37. Karnitz, L.M. & Zou, L. Molecular Pathways: Targeting ATR in Cancer Therapy. *Clin Cancer Res* **21**, 4780-4785 (2015).

38. Sakurikar, N., Thompson, R., Montano, R. & Eastman, A. A subset of cancer cell lines is acutely sensitive to the Chk1 inhibitor MK-8776 as

monotherapy due to CDK2 activation in S phase. *Oncotarget* **7**, 1380-1394 (2016).

39. Hong, D.*, et al.* Phase I Study of LY2606368, a Checkpoint Kinase 1 Inhibitor, in Patients With Advanced Cancer. *J Clin Oncol* **34**, 1764-1771 (2016).

40. Willems, E.*, et al.* The functional diversity of Aurora kinases: a comprehensive review. *Cell Div* **13**, 7 (2018).

41. Staff, S., Isola, J., Jumppanen, M. & Tanner, M. Aurora-A gene is frequently amplified in basal-like breast cancer. *Oncol Rep* **23**, 307-312 (2010).

42. Opyrchal, M.*, et al.* Aurora-A mitotic kinase induces endocrine resistance through down-regulation of ERalpha expression in initially ERalpha+ breast cancer cells. *PLoS One* **9**, e96995 (2014).

43. Haddad, T.C.*, et al.* Phase I trial to evaluate the addition of alisertib to fulvestrant in women with endocrine-resistant, ER+ metastatic breast cancer. *Breast Cancer Res Treat* **168**, 639-647 (2018).

44. Oser, M.G.*, et al.* Cells Lacking the RB1 Tumor Suppressor Gene Are Hyperdependent on Aurora B Kinase for Survival. *Cancer Discov* **9**, 230-247 (2019).

45. Chakravarty, D.*, et al.* OncoKB: A Precision Oncology Knowledge Base. *JCO Precis Oncol* **2017**(2017).

1394 46. Sondka, Z.*, et al.* The COSMIC Cancer Gene Census: describing genetic
1395 dysfunction across all human cancers. *Nat Rev Cancer* **18**, 696-705
1396 (2018).
1397 47. Sanchez-Vega, F.*, et al.* Oncogenic Signaling Pathways in The Cancer
1398 Genome Atlas. *Cell* **173**, 321-337 e310 (2018).
1399 48. Vogelstein, B.*, et al.* Cancer genome landscapes. *Science* **339**, 1546-
1400 1558 (2013).
1401 49. Adalsteinsson, V.A.*, et al.* Scalable whole-exome sequencing of cell-free
1402 DNA reveals high concordance with metastatic tumors. *Nat Commun* **8**,
1403 1324 (2017).
1404 50. Fisher, S.*, et al.* A scalable, fully automated process for construction of
1405 sequence-ready human exome targeted capture libraries. *Genome Biol*
1406 **12**, R1 (2011).
1407 51. Reich, M.*, et al.* GenePattern 2.0. *Nat Genet* **38**, 500-501 (2006).
1408 52. Cibulskis, K.*, et al.* ContEst: estimating cross-contamination of human
1409 samples in next-generation sequencing data. *Bioinformatics* **27**, 2601-
1410 2602 (2011).
1411 53. Cibulskis, K.*, et al.* Sensitive detection of somatic point mutations in
1412 impure and heterogeneous cancer samples. *Nat Biotechnol* **31**, 213-219
1413 (2013).
1414 54. Saunders, C.T.*, et al.* Strelka: accurate somatic small-variant calling from
1415 sequenced tumor-normal sample pairs. *Bioinformatics* **28**, 1811-1817
1416 (2012).

55. Costello, M., *et al.* Discovery and characterization of artifactual mutations in deep coverage targeted capture sequencing data due to oxidative DNA damage during sample preparation. *Nucleic Acids Res* **41**, e67 (2013).

56. Van Allen, E.M., *et al.* Whole-exome sequencing and clinical interpretation of formalin-fixed, paraffin-embedded tumor samples to guide precision cancer medicine. *Nat Med* **20**, 682-688 (2014).

57. Ramos, A.H., *et al.* Oncotator: cancer variant annotation tool. *Hum Mutat* **36**, E2423-2429 (2015).

58. Olshen, A.B., Venkatraman, E.S., Lucito, R. & Wigler, M. Circular binary segmentation for the analysis of array-based DNA copy number data. *Biostatistics* **5**, 557-572 (2004).

59. DePristo, M.A., *et al.* A framework for variation discovery and genotyping using next-generation DNA sequencing data. *Nat Genet* **43**, 491-498 (2011).

60. Wala, J.A., *et al.* SvABA: genome-wide detection of structural variants and indels by local assembly. *Genome Res* **28**, 581-591 (2018).

61. Walsh, R., *et al.* Reassessment of Mendelian gene pathogenicity using 7,855 cardiomyopathy cases and 60,706 reference samples. *Genet Med* **19**, 192-203 (2017).

62. Carter, S.L., *et al.* Absolute quantification of somatic DNA alterations in human cancer. *Nat Biotechnol* **30**, 413-421 (2012).

63. Roth, A., *et al.* PyClone: statistical inference of clonal population structure in cancer. *Nat Methods* **11**, 396-398 (2014).

64. Dang, H.X., *et al.* ClonEvol: clonal ordering and visualization in cancer sequencing. *Ann Oncol* **28**, 3076-3082 (2017).

65. Ulz, P., *et al.* Whole-genome plasma sequencing reveals focal amplifications as a driving force in metastatic prostate cancer. *Nat Commun* **7**, 12008 (2016).

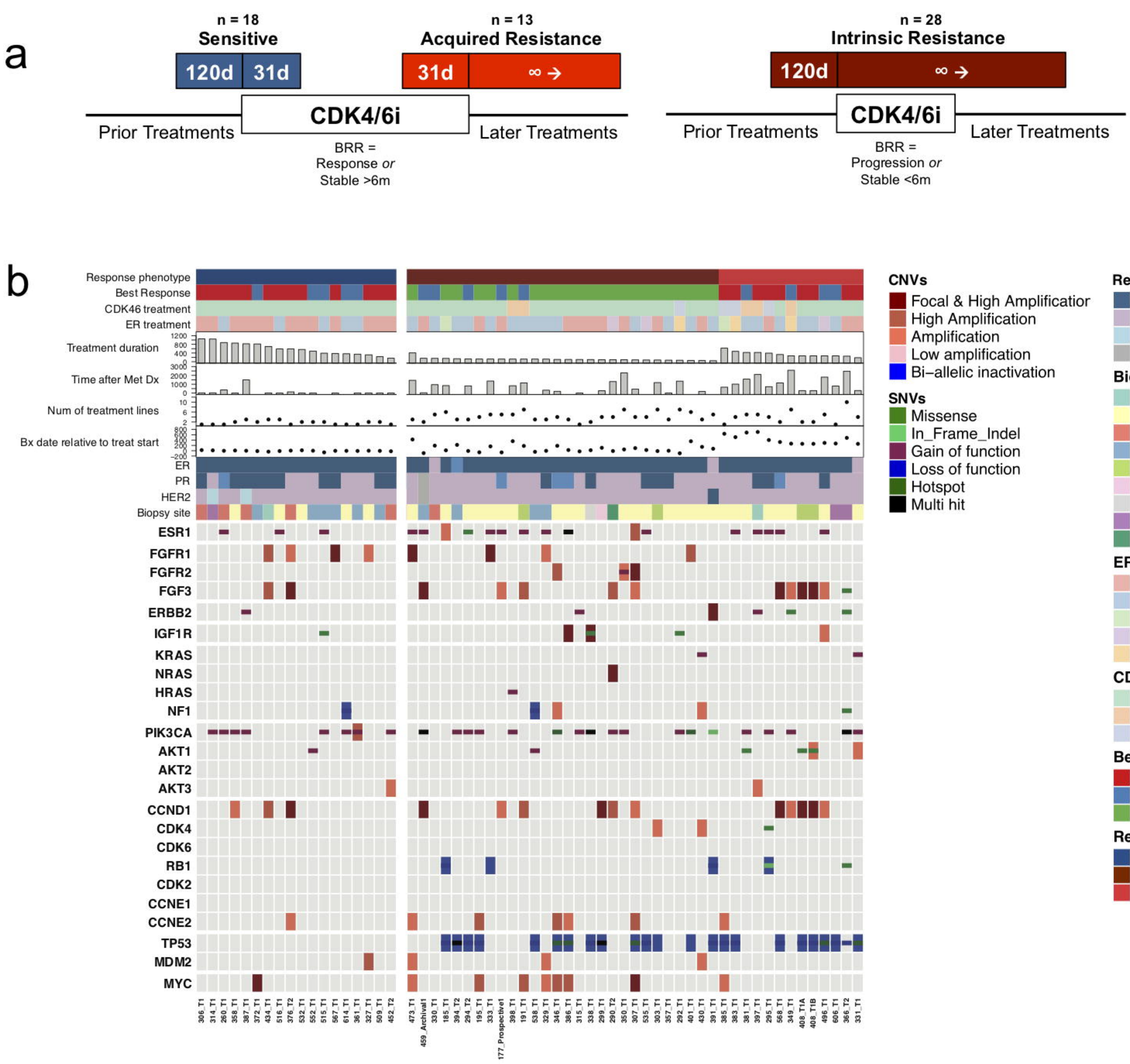

Figure 1. The genomic landscape of CDK4/6i resistance is heterogeneous, with multiple potential driver events.

(a) Biopsy phenotypes were assigned as *sensitive, acquired resistance,* or *intrinsic resistance* based upon timing of the biopsy relative to CDK4/6i exposure (d - days), best radiographic response (BRR), and duration of treatment. Patients were categorized as experiencing clinical benefit on CDK4/6i if interval restaging demonstrated a response or disease stability for at least six months. (b) Mutational matrix (CoMut) depicting the genomic landscape of the CDK4/6i cohort (n = 59 biopsies, 58 patients). Copy number alterations and mutational events in select genes of interest are shown. Clinical parameters (shown at the top) include receptor status, anti-estrogen agent, CDK4/6 inhibitor, best radiographic response (P – progression, R – response, S – stable), biopsy phenotype (S – sensitive, IR – intrinsic resistance, AR – acquired resistance), treatment duration (days), biopsy timing relative to treatment initiation (days), time since metastatic diagnosis (days), and number of lines of prior treatment. (c) Phenotype distribution plot demonstrating a higher frequency of copy number amplifications in Aurora Kinase A (AURKA) among resistant biopsies (AR + IR, left) compared to sensitive biopsies (right, 0.0081, Welch test). (d) Bar plot visualization of mutational (M) and/or copy number alterations (A – amplification, LA – low amplification) in select genes. The proportional enrichment (fraction of samples demonstrating alteration) in sensitive biopsies (left, blue) and resistant biopsies (AR + IR, right, red) is included.

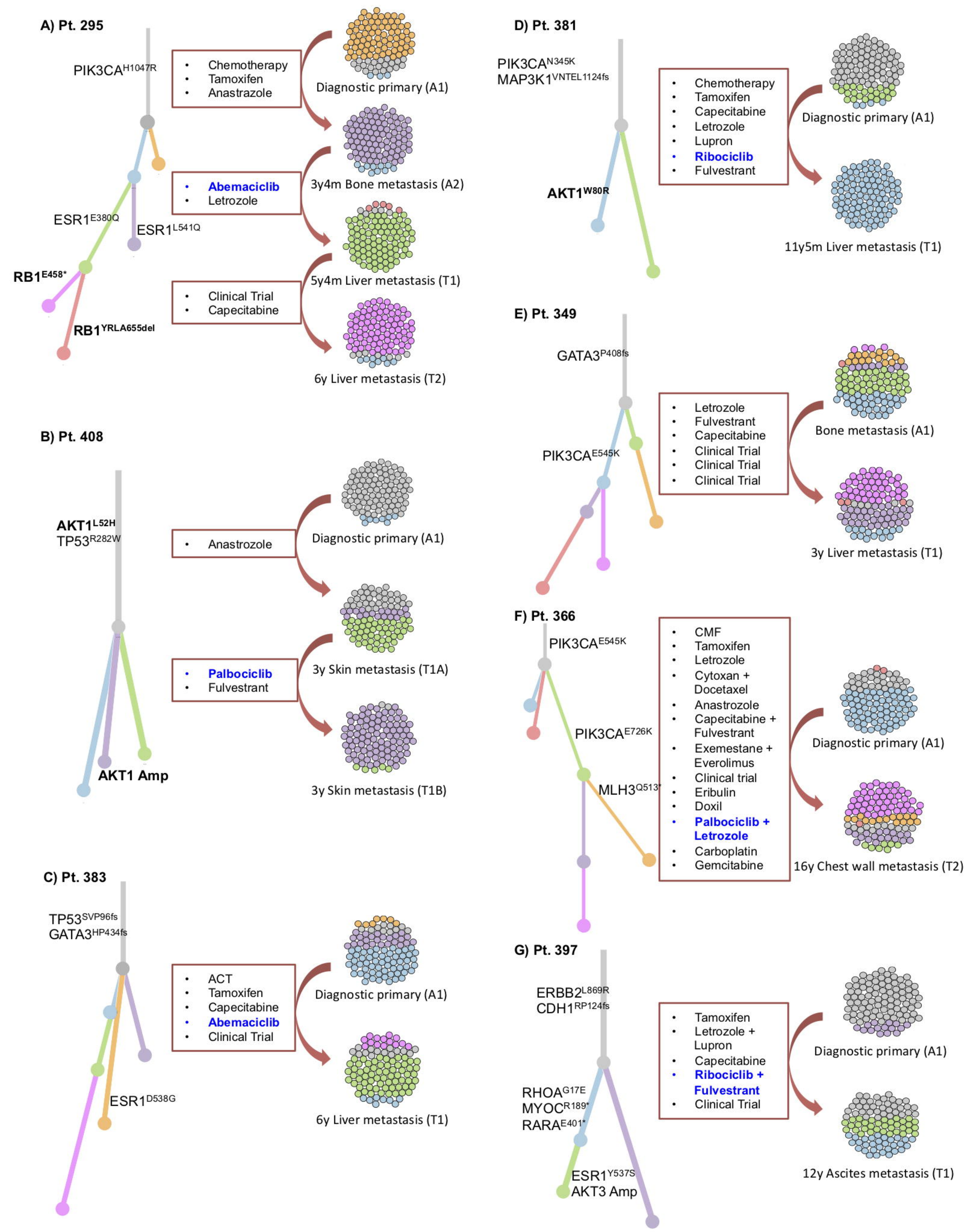

Figure 2. Acquired resistance to CDK4/6i in patients with pre-treatment and post-progression biopsies demonstrates convergent evolution of biallelic RB1 disruption and evolved AKT1 activation.

Phylogenetic analysis depicting the evolutionary history for seven patients with acquired alterations, with clonal evolutionary dynamics demonstrating: (a) acquired polyclonal ESR1 mutations after aromatase inhibition, followed by convergent evolution of RB1 inactivation, with different RB1-inactivating mutations acquired in two parallel sibling clones; (b) Acquired AKT1 amplification; (c) No notable candidate for acquired mechanism of resistance (MOR); (d) Acquired AKT1 (W80R) mutation; (e) No notable candidate for acquired MOR; (f) Acquired inactivation of DNA Mismatch Repair Protein (MLH3); and (g) Acquired activating ESR1 mutation (Y537S) and amplification in AKT3.

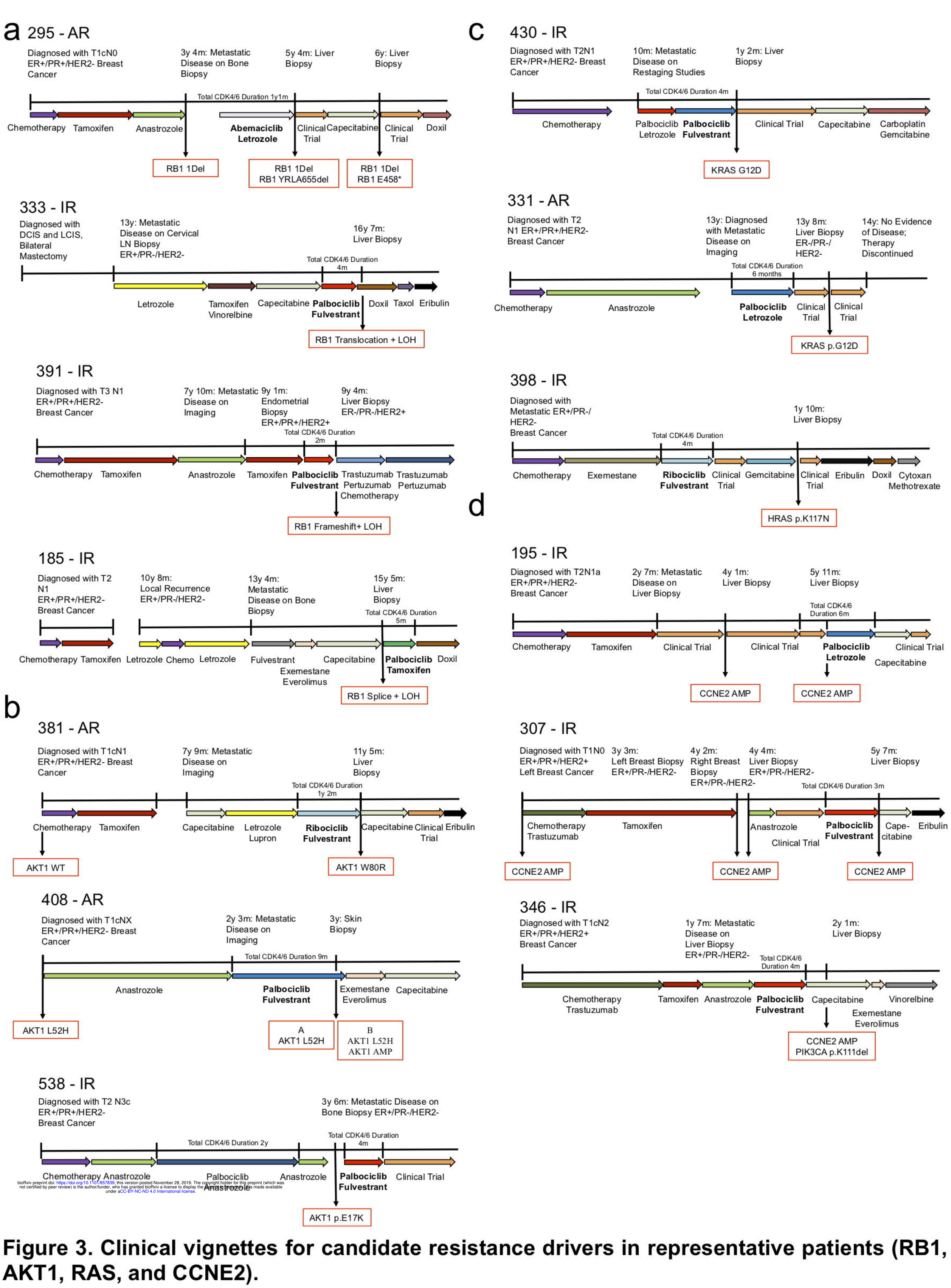

Figure 3. Clinical vignettes for candidate resistance drivers in representative patients (RB1, AKT1, RAS, and CCNE2).

Clinical vignettes including treatment sequence, timing of metastatic progression, and available biopsies with key genomic findings are provided for the following - (a) four patients with biallelic alterations in RB1, including a patient with multiple biopsies and convergent evolution toward RB1 disruption (top, phylogenetic analysis for this patient is provided in Figure 2A). (b) Three patients with acquired alterations in AKT1 following progression on CDK4/6i. In the first (top), a new mutation in AKT1 W80R was identified. In the second (middle), a baseline alteration (AKT1 L52H) was identified at the time of diagnosis; at the time of progression on CDK4/6i, two biopsies were obtained – both demonstrating the baseline AKT1 L52H mutation, one also demonstrating an acquired amplification of the wild-type AKT1 protein (phylogenetic analyses for these patients are provided in Figure 2B and D). (c) Three patients with resistance to CDK4/6i and RAS-family alterations (including two instances of KRAS G12D and one instance of HRAS mutation). (d) Three patients with intrinsic resistance to CDK4/6i and amplification events in CCNE2.

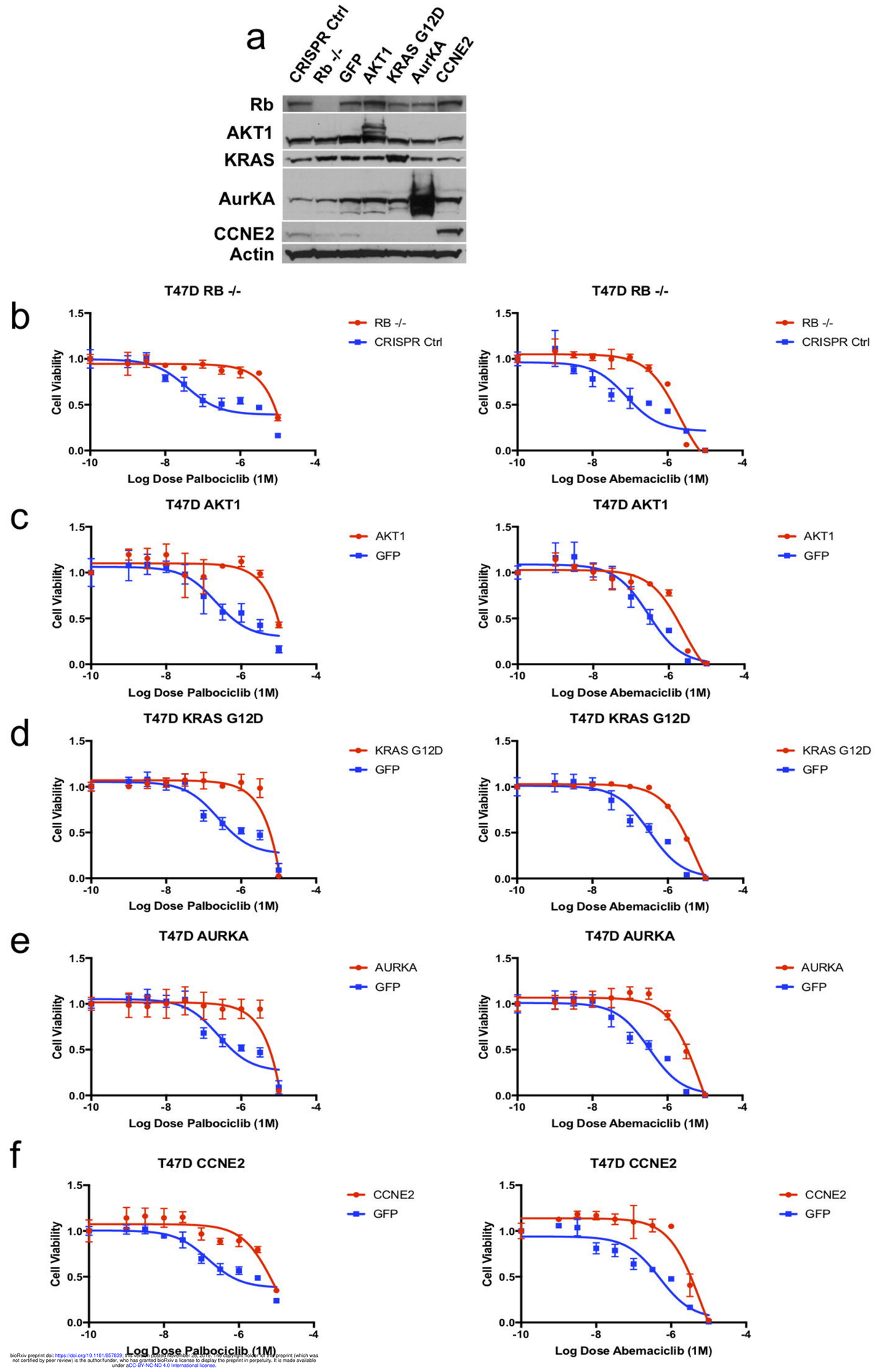

Figure 4. Candidate genomic alterations provoke CDK4/6i resistance *in vitro*.

(a) T47D cells were modified via CRISPR-mediated downregulation (RB1) or lentiviral overexpression (AKT1, KRAS G12D, AURKA, CCNE2) to interrogate potential resistance mediators identified in patient biopsy samples. Western blotting with the indicated antibodies is included. (b-f) Modified T47D cells were exposed to escalating doses of CDK4/6i (palbociclib – left, abemaciclib – right) and viability was estimated via cell-titer-glo (CTG) assay. Control (CRISPR non-targeting guide or GFP) cells are plotted along with the resistance driver of interest (RB1 – b, AKT1 – c, KRAS G12D – d, AURKA – e, CCNE2 – f). Parental and variant cell lines are normalized to vehicle control and viability is plotted as a function of increasing CDK4/6i (graphed as triplicate average +/- standard deviation). All variants provoke CDK4/6i resistance (to both palbociclib and abemaciclib) *in vitro* in T47D cells. Corresponding IC50 values are included in Supplemental Table 7.

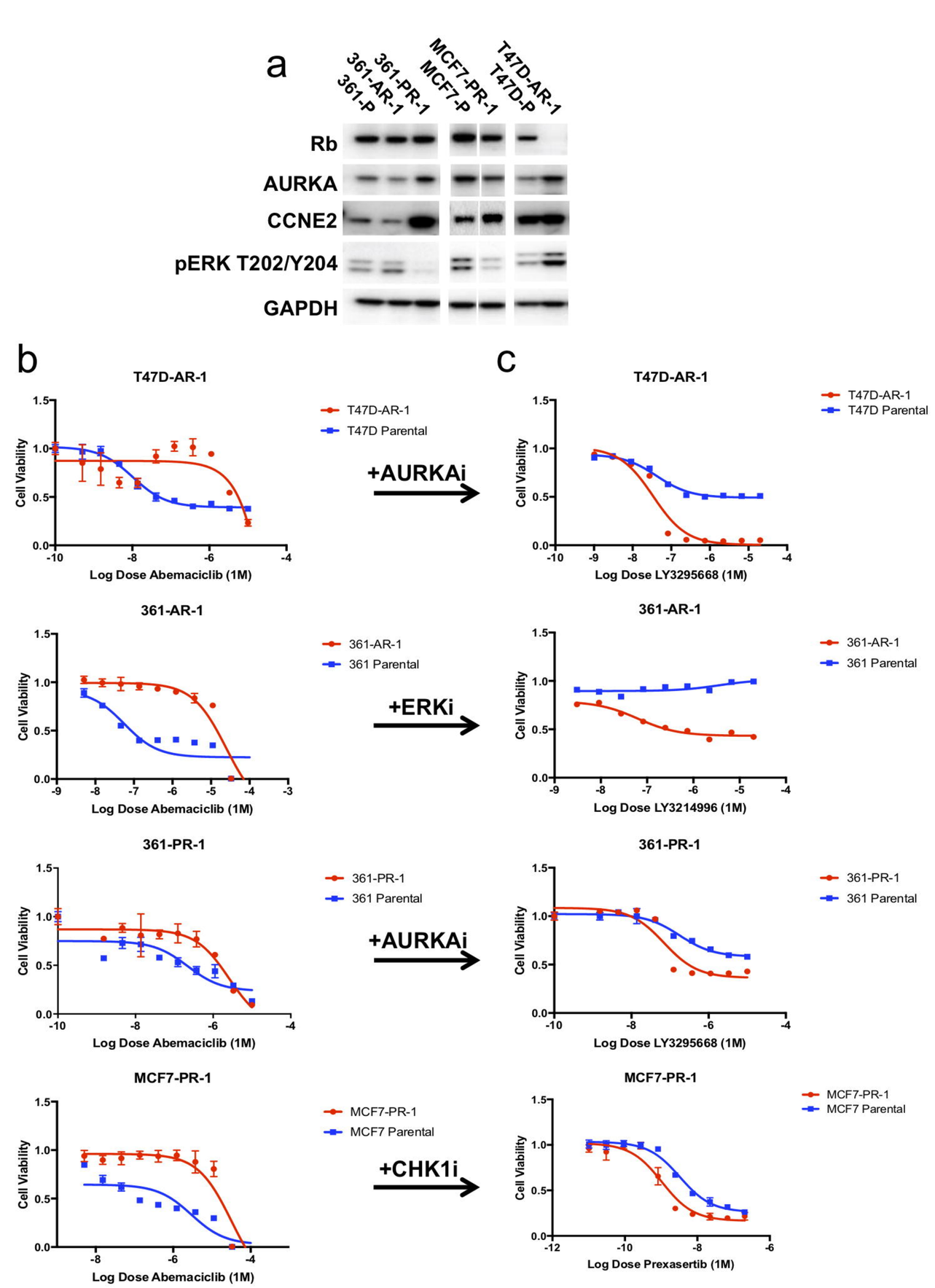

Figure 5. Candidate mutations emerge in cell lines cultured under CDK4/6i selective pressure and define new therapeutic dependencies *in vitro*.

(a) Breast cancer cell lines (T47D, MCF7, MDA-MB-361) were cultured long-term to resistance in the presence of CDK4/6i (palbociclib, abemaciclib). The resulting cell lines which emerged were subjected to western blotting for putative mediators of drug resistance (RB1, AKT1, KRAS/ERK, AURKA, and CCNE2). (b-c) T47D cells cultured to resistance in the presence of abemaciclib demonstrated low levels of RB1 expression (T47D-AR1) and increased sensitivity to the AURKA inhibitor LY3295668. MDA-MB-361 cells cultured to resistance in the presence of abemaciclib demonstrated high levels of ERK activation (361-AR1) and increased sensitivity to the ERK inhibitor LY3214996. MDA-MB-361 cells cultured to resistance in the presence of palbociclib demonstrated high levels of AURKA (361-PR1) and increased sensitivity to the AURKA inhibitor LY3295668. MCF7 cells cultures to resistance in the presence of palbociclib demonstrated increased levels of CCNE2 (MCF7-PR1) and increased sensitivity to the CHEK1 inhibitor prexasertib.

a

Baseline Pre-

Interval Restaging

Interval Restaging

+5m

+7m

Diagnosed with Stage IIIC HR+/HER2- Breast Cancer

2y 5m: Metastatic Progression

Total CDK4/6 Duration 3y 8m

Total AURKi Duration ~11m

Chemotherapy

Tamoxifen

Palbociclib
Letrozole

LY3295668

Ki67 (10x)

RB1 (10x)

b

Patients with metastatic ER+ breast cancer resistance to CDK4/6 inhibitor

TUMOR GENOMIC PROFILING OF RESISTANT METASTATIC TUMOR BIOPSY OR ctDNA

RB1 Loss

AURKA Amplification

ERBB2 Activation

FGFR2 Activation

RAS Activation

AKT1 Activation

CCNE2 Amplification

AURKA Inhibitor

AURKA Inhibitor

HER2 Inhibitor

FGFR Inhibitor

ERK Inhibitor

AKT1 Inhibitor

CHK1 Inhibitor

+/- CDK4/6 inhibitor
+/- SERD/SERM

AURKA

MAPK Pathway

AKT/MTOR

CDK2/CCNE

Figure 6. A novel aurora kinase A inhibitor demonstrates therapeutic efficacy in a patient with metastatic HR+ breast cancer after progression on CDK4/6i.

(a) A patient with locally advanced HR+/HER2- breast cancer developed metastatic progression on adjuvant tamoxifen. She received CDK4/6i and letrozole in the first line setting with prolonged clinical benefit (>3 years). At progression, she was placed on trial with the AURKA inhibitor LY3295668; she subsequent experienced prolonged disease control ~11 months). Baseline staging studies following progression on CDK4/6i in the patient described are included (top); she had osseous metastatic disease and visceral disease was limited to the foci noted in the liver. Two interval restaging studies (top) demonstrate disease stability/mild response. Liver biopsy obtained at the time of progression on CDK4/6i and prior to LY3295668 demonstrated high Ki67 and high RB1 protein expression via immunohistochemistry (IHC, 10x) (bottom). (b) Schematic diagram demonstrating the potential utility of next-generation sequencing following progression on CDK4/6i; actionable alterations in RB1, ERBB2, FGFR2, AKT1, RAS, AURKA, and CCNE2 could dictate informed selection of targeted therapies as indicated.